Two-Pore-Domain Potassium (K$_{2P}$-) Channels: Cardiac Expression Patterns and Disease-Specific Remodelling Processes

Felix Wiedmann [1,2,3] [iD], **Norbert Frey** [1,2,3] **and Constanze Schmidt** [1,2,3,*]

1 Department of Cardiology, University of Heidelberg, 69120 Heidelberg, Germany;
Felix.Wiedmann@med.uni-heidelberg.de (F.W.); norbert.frey@med.uni-heidelberg.de (N.F.)

2 DZHK (German Center for Cardiovascular Research), Partner Site Heidelberg/Mannheim, University of Heidelberg, 69120 Heidelberg, Germany

3 HCR, Heidelberg Center for Heart Rhythm Disorders, University of Heidelberg, 69120 Heidelberg, Germany

* Correspondence: Constanze.Schmidt@med.uni-heidelberg.de; Tel.: +49-6221-568187; Fax: +49-6221-565724

Abstract: Two-pore-domain potassium (K$_{2P}$-) channels conduct outward K$^+$ currents that maintain the resting membrane potential and modulate action potential repolarization. Members of the K$_{2P}$ channel family are widely expressed among different human cell types and organs where they were shown to regulate important physiological processes. Their functional activity is controlled by a broad variety of different stimuli, like pH level, temperature, and mechanical stress but also by the presence of lipids or pharmacological agents. In patients suffering from cardiovascular diseases, alterations in K$_{2P}$-channel expression and function have been observed, suggesting functional significance and a potential therapeutic role of these ion channels. For example, upregulation of atrial specific K$_{2P}$3.1 (TASK-1) currents in atrial fibrillation (AF) patients was shown to contribute to atrial action potential duration shortening, a key feature of AF-associated atrial electrical remodelling. Therefore, targeting K$_{2P}$3.1 (TASK-1) channels might constitute an intriguing strategy for AF treatment. Further, mechanoactive K$_{2P}$2.1 (TREK-1) currents have been implicated in the development of cardiac hypertrophy, cardiac fibrosis and heart failure. Cardiovascular expression of other K$_{2P}$ channels has been described, functional evidence in cardiac tissue however remains sparse. In the present review, expression, function, and regulation of cardiovascular K$_{2P}$ channels are summarized and compared among different species. Remodelling patterns, observed in disease models are discussed and compared to findings from clinical patients to assess the therapeutic potential of K$_{2P}$ channels.

Keywords: K$_{2P}$-channel; TASK-1; TREK-1; two-pore-domain potassium channel

1. Introduction

Two-pore-domain potassium (K$_{2P}$) channels are expressed throughout the human body and contribute to background potassium conductance in many different cell types [1,2]. In the human genome 15 K$_{2P}$ channels have been described which differ from classical potassium channels by the fact that each subunit carries two pore-forming domains, and the channels thus assemble as dimers instead of tetramers (Figure 1). K$_{2P}$ channels give rise to background or "leak" potassium currents which control a multitude of physiological processes [1]. Initially, K$_{2P}$ currents were described as outward rectifying "leakage currents" but recent work has shown that several members of the K$_{2P}$ family can also be voltage activated [3].

K$_{2P}$ currents show a high degree of similarity to the potassium plateau currents I_{KP}, described in guinea-pig cardiomyocytes and the steady-state potassium current $I_{K,SS}$, characterized in murine cardiomyocytes and the arachidonic acid-sensitive potassium current I_{KAA} from rat ventricular cardiomyocytes [4–7]. Cardiac mRNA abundance was described for several members of the K$_{2P}$ family (Figure 2) In the present review, expression,

function, and regulation of cardiovascular K_{2P} channels are summarized and compared among different species. Remodelling patterns, observed in disease models are discussed and compared to findings from clinical patients to assess the therapeutic potential of K_{2P} channels (Figure 3).
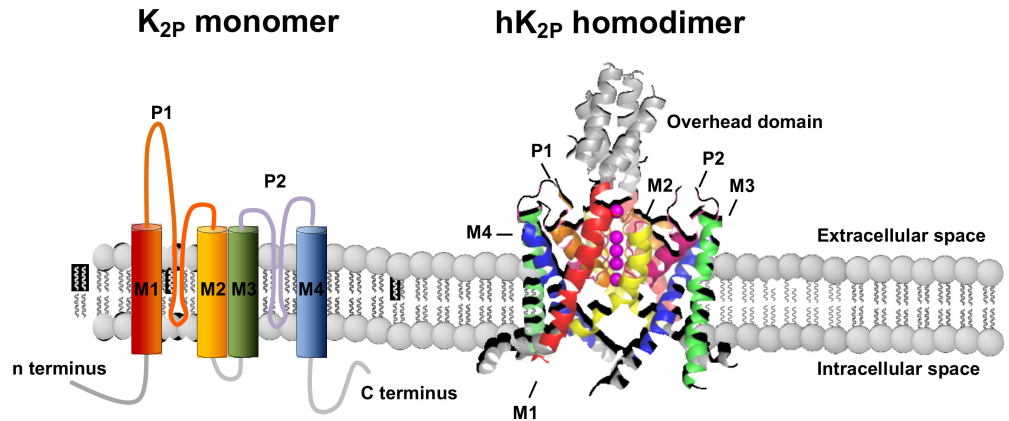
Figure 1. Membrane topology and structure of K_{2P} channels. K_{2P} channel monomers (**left**), consisting of 4 transmembrane domains (M1–4) and 2 pore forming loops (P1–2) assemble as homo- or heterodimers. (**right**).
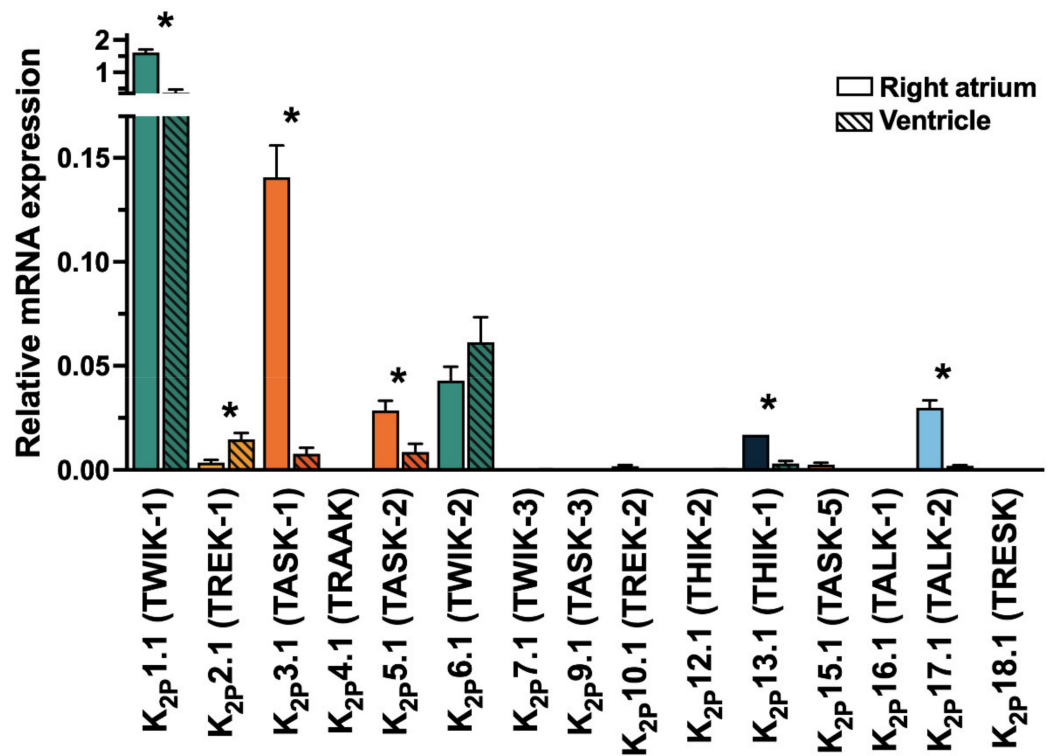
Figure 2. Cardiac mRNA levels of K_{2P} channels in the human heart (whole tissue). Expression of two-pore-domain potassium (K_{2P}-) channel mRNA level in human right atrial (*n* = 10) and left ventricular (*n* = 5) tissue samples. Data are given as mean ± SEM relative to the housekeeping gene importin 8 (*IPO8*). * indicate *p* < 0.05 from Student's t-tests. Data from Schmidt et al. 2015, Circulation [8].

Figure 3. Potential translational implications of cardiac K2P channel expression.AF, atrial fibrillation; OSAS, obstructive sleep apnea; PAH pulmonary arterial hypertension; RVOT, right ventricular outflow tract; VF, ventricular fibrillation.
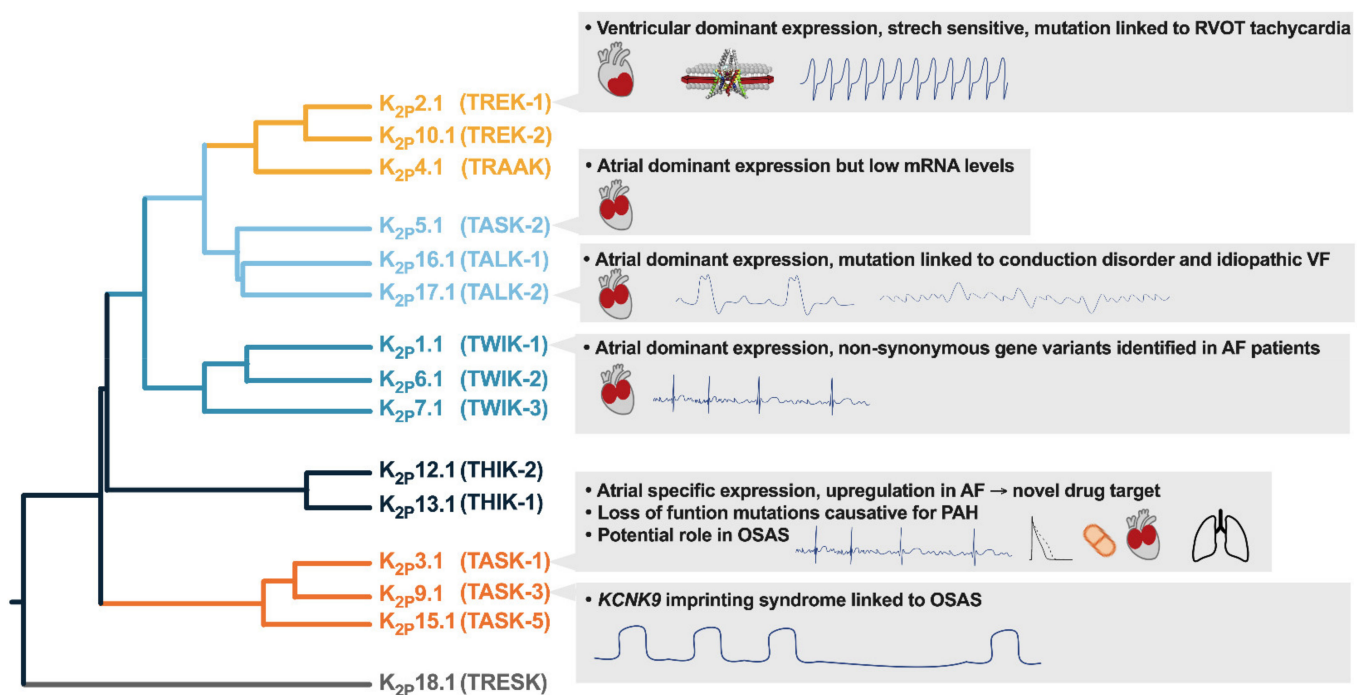
2. Structural Assembly and Nomenclature of K_{2P} Channels

The 15 channel subunits of the K_{2P} family each consists of around 300 and 550 amino acids. The sequence differences between the individual subunits of the K_{2P} channel can sometimes be as large as to other potassium channel families. $K_{2P}18.1$ (TRESK) channel subunits, for example share only 19% amino acid sequence identity with the other K_{2P} family members. But the common feature that links them is the eponymous structural motif of two pore-forming domains per subunit, which distinguishes them from all other potassium channel groups. As shown in Figure 1, the four alphahelical transmembrane domains (M1–M4) flank two pore-forming loops (P1 and P2), each containing the potassium selective filter motif (GLG, GFG, or GYG). M1 and P1 are connected by a long extracellular loop, forming an overhead cap structure. The short amino terminus and a much longer carboxy terminus, which contains a variety of regulatory phosphorylation and protein interaction motifs, are localized intracellularly. Whereas most potassium channels form tetramers with one pore-forming loop per subunit, a functional two-pore domain potassium channel is composed of two alpha subunits (Figure 1). In addition to homodimerization, certain K_{2P} channel subunits can also assemble as heterodimers. This is mainly described within the same subfamilies (i.e., TASK-1/TASK-3, TREK-1/TRAAK, THIK-1/THIK-2), but can also occur between TWIK-1 and TREK or TASK-1, and between TASK-1/TALK-2 subunits. Physiological relevance in the perception of hypoxia has been described for TASK-1/TASK-3 heterodimers and TWIK-1/TREK-1 heterodimers have been detected in astrocytes. Apart from the TASK-1 and TALK-1 subfamilies, all K_{2P} channel subunits possess a conserved Cys-amino acid residue of the overhead domain that is thought to play a major, although not yet conclusively elucidated, role in dimerization. The predicted membrane topology and tertiary structure have already been confirmed by X-ray structural analysis for several K_{2P}-channels (Table 1).

Table 1. Nomenclature of K_{2P}-channels.
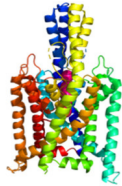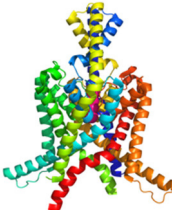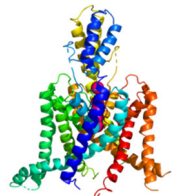
Gene Name	IUPHAR K_{2P} Nomenclature	Functional Name	Other Names	Crystal Structure
KCNK1	$K_{2P}1.1$	TWIK-1 (Tandem of P-domains in a weak inward-rectifying K^+ channel 1)	hOHO, DPK, KCNO1	
KCNK2	$K_{2P}2.1$	TREK-1 (TWIK-related K^+ channel 1)	TPKC1	
KCNK3	$K_{2P}3.1$	TASK-1 (TWIK-related acid-sensitive K^+ channel 1)	TBAK-1, OAT-1, PPH4	
KCNK4	$K_{2P}4.1$	TRAAK (TWIK-related arachidonic acid activated K^+ channel)	FHEIG	
KCNK5	$K_{2P}5.1$	TASK-2 (TWIK-related acid-sensitive K^+ channel 2)		
KCNK6	$K_{2P}6.1$	TWIK-2 (Tandem of P-domains in a weak inward-rectifying K^+ channel 2)	TOSS	-
KCNK7	$K_{2P}7.1$	TWIK-3 (Tandem of P-domains in a weak inward-rectifying K^+ channel 3)		-
The name *kcnk8* was initially given to a murine K_{2P} gene which was later identified as an ortholog of the human *KCNK7* gene and therefore renamed to *kcnk7*				
KCNK9	$K_{2P}9.1$	TASK-3 (TWIK-related acid-sensitive K^+ channel 3)	KT3.2, BIBARS, TASK32	-

Gene Name	IUPHAR K$_{2P}$ Nomenclature	Functional Name	Other Names	Crystal Structure
KCNK10	K$_{2P}$10.1	TREK-2 (TWIK-related K$^+$ channel 2)	PPP1R97	
KCNK11 was withdrawn due to nomenclature duplications with *KCNK15*				
KCNK12	K$_{2P}$12.1	THIK-2 (Tandem pore domain halothane inhibited K$^+$ channel 2)		-
KCNK13	K$_{2P}$13.1	THIK-1 (Tandem pore domain halothane inhibited K$^+$ channel 1)		-
KCNK14 was withdrawn due to nomenclature duplications with *KCNK15*				
KCNK15	K$_{2P}$15.1	TASK-5 (TWIK-related acid-sensitive K$^+$ channel 5)	KT3.3, dJ781B1.1	-
KCNK16	K$_{2P}$16.1	TALK-1 (TWIK-related alkaline pH-activated K$^+$ channel 1)		-
KCNK17	K$_{2P}$17.1	TALK-2 (TWIK-related alkaline pH-activated K$^+$ channel 2)	TASK-4	-
KCNK18	K$_{2P}$18.1	TRESK (TWIK-related spinal cord K$^+$ channel 1)	MGR13, TRIK, TRESK2	-

IUPHAR, International Union of Basic and Clinical Pharmacology. Visualizations of the channel structurs were generated with PyMOL (TM) Molecular Graphics System, Version 2.3.0 (Schrodinger, LLC; New York, NY, USA) from crystall stuctures with the protein database enty numbers: 3UKM, 4TWK, 6RV2, 3UM7, 6WLV, 3UX0 and 4BW5.

Upon their discovery, the individual K$_{2P}$-channels received trivial names reflecting their respective structural and regulatory properties: TWIK: "Tandem of P domains in a weak inward rectifying K$^+$ channel", TREK: "TWIK-related K$^+$ channel", TASK: "TWIK-related acid-sensitive K$^+$ channel", TRAAK: "TWIK-related arachidonic acid activated K$^+$ channel", TALK "TWIK-related alkaline pH-activated K$^+$ channel", THIK "tandem pore domain halothane-inhibited K$^+$ channel", and TRESK "TWIK-related spinal cord K$^+$ channel". In parallel, the channels are labeled consecutively with the designations K$_{2P}$1.1 to K$_{2P}$18.1 according to the Human Genome Organization name of the encoding gene (*KCNK1* to *KCNK18*) (see Figure 2 and Table 1). Each of the 15 subfamilies members (K$_{2P}$1.1 to K$_{2P}$18.1) contains only one member. Unfortunately, this led to a confusing nomenclature in which channels with different functional properties such as TASK-1 and TASK-2 have similar names, while other channels are titled with acronyms of factually incorrect names (for example, TWIK-1 is not a weak inward rectifier but an open rectifier). Further, some channels carry a variety of redundant names such as in case of K$_{2P}$3.1: TBAK1, TASK1 and OAT1. Several *KCNKx* designators were initially assigned to K$_{2P}$ channel transcripts that later turned out to be orthologs of other human K$_{2P}$ channels. Thus, *KCNK8* (the murine transcript designated *kcnk8* later proved to be an ortholog of human *KCNK7* and was therefore renamed *kcnk7*), *KCNK11*, and *KCNK14* (both orthologs

of *KCNK15*) do not exist [9]. For better understanding, we will provide the trivial names of the channel subunits in brackets in addition to the International Union of Basic and Clinical Pharmacology IUPHAR (K_{2P}X.1) names. Since they do not show any functional activity in heterologous expression systems, the channels *KCNK7*, *KCNK12* and *KCNK15* are referred to as silent K_{2P} channels. It remains unclear whether these K_{2P} channel subunits are truly nonfunctional in vivo or whether they just lack essential cofactors to achieve functionality upon heterologous expression. In fact, the functionality of the K_{2P}16.1 channels could be restored by deletion of an n-terminal ER-retention motif [8].

3. K_{2P}1.1 (TWIK-1)

Robust cardiac mRNA levels were consistently described for *KCNK1* [10–15]. In a study from our laboratory, which examined the expression of all K_{2P} channels in the human heart (TaqMan-qPCR; Figure 2), the highest mRNA levels were detected for *KCNK1* [10]. Atrial predominant mRNA abundance was shown in patient-derived tissue samples but not in rodents (Table 2) [10,16].

Table 2. Evidence in literature for cardiac expression of K_{2P} channel subunits at mRNA or protein level in different species.

K_{2P} Channel Subunit	Species	Protein /mRNA	Observation	Citation
K_{2P}1.1 (TWIK-1)	Zebrafish	mRNA (RT-PCR, ISH)	Ubiquitous *kcnk1a* and *kcnk1b* ortholog mRNA in embryonic heart	[11]
	Mouse	mRNA (RT-PCR)	No cardiac mRNA abundance	[17]
	Mouse	mRNA (RT-qPCR, TaqMan)	Moderate cardiac mRNA abundance, V > A	[16]
	Rat	mRNA (RT-PCR)	Moderate cardiac mRNA abundance, A > V	[18]
	Rat	mRNA (RT-PCR)	Moderate cardiac mRNA abundance	[15]
	Rat	mRNA (RT-qPCR, TaqMan)	Cardiac mRNA abundance mRNA detected in sinoatrial tissue	[19]
	Human	mRNA (NB)	Cardiac mRNA abundance	[20]
	Human	mRNA (RT-PCR)	Cardiac mRNA abundance, V > A	[21]
	Human	mRNA (RT-qPCR, TaqMan)	Cardiac mRNA abundance, A > V Highest mRNA level among all K_{2P} channels	[10]
	Human	mRNA (RT-qPCR)	Cardiac mRNA abundance, A>V	[13]
	Human	mRNA (RT-qPCR)	mRNA detected in human ventricular tissue mRNA detected in iPS-derived cardiomyocytes	[22]
	Human	mRNA (RT-qPCR, TaqMan)	Cardiac mRNA abundance	[23]
	Human	mRNA (Affymetrix chip and RT-qPCR, TaqMan)	Cardiac mRNA abundance, A > Purkinje fibers > V	[12]
	Human	mRNA (Affymetrix chip, RT-qPCR, TaqMan) and protein (WB)	Cardiac mRNA abundance, A > Purkinje fibers > V Cardiac protein expression, A > V	[14]
K_{2P}2.1 (TREK-2)	Mouse	mRNA (NB)	Cardiac mRNA abundance	[24]
	Mouse	mRNA (RT-PCR)	Cardiac mRNA abundance, V > A	[17]
	Mouse	mRNA (RT-PCR)	Cardiac mRNA abundance	[25]
	Mouse	mRNA (RT-qPCR) and protein (WB)	Cardiac mRNA abundance, V > A Cardiac protein expression	[26]

Table 2. *Cont.*

K₂ₚ Channel Subunit	Species	Protein /mRNA	Observation	Citation
	Mouse	mRNA (RT-qPCR, TaqMan)	Cardiac mRNA levels, V > A	[16]
	Mouse	Protein (IF)	Protein expression in isolated ventricular cardiomyocytes	[27]
	Rat	mRNA (RT-PCR)	mRNA abundance in isolated ventricular cardiomyocytes	[28]
	Rat	mRNA (RT-PCR)	Cardiac mRNA abundance, A and V	[18]
	Rat	mRNA (RT-PCR)	Cardiac mRNA abundance, A and V	[29]
	Rat	mRNA (RT-PCR)	Endocardial mRNA levels > epicardial mRNA expression	[30]
	Rat	mRNA (RT-PCR)	Cardiac mRNA levels, mRNA detected in cardiomyocytes	[15]
	Rat	mRNA (RT-PCR)	Cardiac mRNA abundance	[31]
	Rat	mRNA (RT-qPCR)	Cardiac mRNA abundance Cardiac mRNA adult heart > fetal heart	[18]
	Rat	mRNA (RT-qPCR, TaqMan)	Cardiac mRNA abundance in sinoatrial tissue	[19]
	Rat	mRNA (RT-PCR)and protein (IF)	Cardiac mRNA abundance, A and V Protein expression in isolated cardiomyocytes	[32]
	Rat	mRNA (RT-PCR) and protein (IF)	mRNA and protein expression in rat cardiomyocytes	[33]
	Rat	mRNA (RT-PCR) and protein (WB, IF)	Cardiac mRNA and protein expression, A and V	[34]
	Rabbit, mouse	Protein (WB)	Cardiac protein expression, SAN > A > V	[35]
	Pig	mRNA (RT-qPCR, TaqMan) and protein (WB)	Cardiac mRNA and protein expression, V = A mRNA and protein expression in sinoatrial and atrioventricular node	[36]
	Pig, human	mRNA (RT-qPCR, TaqMan)	Atrial mRNA expression in human and pig	[37]
	Human	mRNA (RT-PCR)	Cardiac mRNA abundance	[31]
	Human	mRNA (RT-qPCR)	Low cardiac mRNA abundance	[38]
	Human	mRNA (RT-qPCR)	Low cardiac mRNA abundance	[39]
	Human	mRNA (RT-qPCR)	Cardiac mRNA abundance, V Low mRNA abundance in iPS-derived cardiomyocytes	[22]
	Human	mRNA (RT-qPCR)	Cardiac mRNA abundance	[39]
	Human	mRNA (RT-qPCR, TaqMan)	Cardiac mRNA abundance, V > A	[10]
	Human	mRNA (RT-qPCR, TaqMan)	Low cardiac mRNA abundance	[23]
	Human	mRNA (RT-qPCR, TaqMan)	Cardiac mRNA levels, V > A	[40]
	Human, mouse	mRNA (RT-qPCR, TaqMan) and protein (WB)	Cardiac mRNA and protein expression in human and mice, V > A	[41]
	Human	Protein (WB)	Cardiac protein expression	[42]
	Human	Protein (WB)	Cardiac protein expression	[43]

Table 2. *Cont.*

K_{2P} Channel Subunit	Species	Protein /mRNA	Observation	Citation
$K_{2P}3.1$ *(TASK-1)*	Chicken embryo	mRNA (ISH) and protein (IF)	Cardiac mRNA and protein expression in chicken embryos	[44]
	Mouse, human	mRNA (NB)	Human and Mouse: Cardiac mRNA abundance	[45]
	Mouse	mRNA (RT-PCR)	Cardiac mRNA abundance	[17]
	Mouse	mRNA (RT-qPCR)	Cardiac mRNA levels, V > A	[26]
	Mouse	mRNA (RT-PCR) and protein (WB)	Cardiac protein expression	[25]
	Mouse, human	mRNA (RT-qPCR, TaqMan)	Cardiac mRNA expression	[46]
	Mouse	mRNA (RT-qPCR, TaqMan) and protein (WB)	Cardiac mRNA and protein expression, A and V	[16]
	Rat	mRNA (RT-qPCR, TaqMan)	Cardiac mRNA abundance in sinoatrial tissue	[19]
	Rat	mRNA (NB, RT-PCR)	Cardiac mRNA abundance, A and V	[47]
	Rat	mRNA (RT-PCR)	Cardiac mRNA abundance, cardiomyocyte mRNA abundance	[15]
	Rat	mRNA (RT-PCR)	Cardiac mRNA abundance	[48]
	Rat	mRNA (RT-PCR)	Cardiac mRNA abundance, A > V	[18]
	Rat, guinea pig, human	mRNA (RT-qPCR, TaqMan)	Human: Cardiac mRNA levels, V > A Rat: Cardiac mRNA abundance, A and V Guinea pig: Cardiac mRNA levels, V > A	[49]
	Dog	Protein (WB)	Atrial protein expression	[50]
	Pig	mRNA (RT-qPCR, TaqMan) and protein (WB)	Cardiac mRNA and protein expression mRNA abundance in sinoatrial and atrioventricular node	[51]
	Pig	mRNA (RT-qPCR, TaqMan) and protein (WB)	Cardiac mRNA and protein expression	[52]
	Human	mRNA (RT-qPCR)	Low cardiac mRNA abundance	[38]
	Human	mRNA (RT-qPCR)	mRNA abundance in Purkinje fibers	[5]
	Human	mRNA (RT-qPCR)	Cardiac mRNA abundance, A > V Cardiac mRNA adult heart > fetal heart	[39]
	Human	mRNA (RT-qPCR)	Low mRNA abundance in human ventricular tissue mRNA abundance in iPS-derived cardiomyocytes	[22]
	Human	mRNA (RT-qPCR, TaqMan)	mRNA levels in isolated atrial cardiomyocytes > in isolated atrial fibroblasts	[53]
	Human	mRNA (RT-qPCR, TaqMan)	Cardiac mRNA abundance	[23]
	Human	mRNA (RT-qPCR, TaqMan)	Cardiac mRNA levels, A > V	[54]
	Human	mRNA (Affymetrix chip and RT-qPCR, TaqMan)	Cardiac mRNA abundance, A	[55]
	Human	mRNA (Affymetrix chip and RT-qPCR, TaqMan)	Cardiac mRNA levels, A > V Expression in Purkinje fibers	[14]

Table 2. *Cont.*

K$_{2P}$ Channel Subunit	Species	Protein /mRNA	Observation	Citation
	Human	mRNA (Affymetrix chip and RT-qPCR, TaqMan)	Cardiac mRNA expression, A > V	[12]
	Human	mRNA (RT-qPCR) and protein (IF)	Cardiac mRNA and protein expression	[56]
	Human	mRNA (RT-qPCR, TaqMan) and protein (WB)	Cardiac mRNA levels, A > V Cardiac protein expression, A	[40]
	Human	mRNA (RT-qPCR, TaqMan) and protein (WB)	Cardiac mRNA levels, A > V Cardiac protein expression, A	[10]
	Human	mRNA (bulk RNAseq)	Cardiac mRNA levels, A > V	[57]
	Mouse	mRNA (RT-PCR, NB)	No cardiac mRNA detectable	[58]
	Mouse	mRNA (RT-qPCR)	Human: no cardiac mRNA detectable Mouse: Low cardiac mRNA abundance, A > V	[41]
	Mouse	mRNA (qRT-PCR) and protein (WB)	Cardiac mRNA abundance	[26]
K$_{2P}$4.1 (TRAAK)	Mouse	mRNA (RT-qPCR, TaqMan)	No cardiac mRNA levels detectable	[16]
	Rat	mRNA (RT-PCR)	No cardiac mRNA levels	[15]
	Rat	mRNA (RT-PCR)	Low cardiac mRNA levels, A and V	[18]
	Human	mRNA (RT-qPCR)	mRNA abundance in human ventricular tissue mRNA abundance in iPS-derived cardiomyocytes	[22]
	Human	mRNA (RT-qPCR)	Low cardiac mRNA levels	[59]
	Human	mRNA (RT-qPCR, TaqMan)	Very low cardiac mRNA levels	[10]
	Human	mRNA (RT-qPCR, TaqMan)	No cardiac mRNA abundance	[23]
	Mouse	mRNA (RT-PCR)	Cardiac mRNA abundance	[17]
	Mouse	mRNA (RT-PCR)	Cardiac mRNA levels, A and V	[26]
	Mouse	mRNA (RT-PCR)	Low cardiac mRNA abundance	[25]
	Mouse	mRNA (RT-qPCR, TaqMan)	Cardiac mRNA levels, A > V	[16]
	Rat	mRNA (NB)	No cardiac mRNA abundance	[60]
	Rat	mRNA (RT-PCR)	Low cardiac mRNA levels, A and V	[18]
K$_{2P}$5.1 (TASK-2)	Rat	mRNA (RT-qPCR, TaqMan)	Cardiac mRNA abundance in sinoatrial tissue	[19]
	Human	mRNA (RT-PCR)	Cardiac mRNA abundance	[61]
	Human	mRNA (RT-qPCR, TaqMan)	Cardiac mRNA abundance	[23]
	Human	mRNA (RT-qPCR)	mRNA abundance in human ventricular tissue mRNA abundance in iPS-derived cardiomyocytes	[22]
	Human	mRNA (RT-qPCR)	Cardiac mRNA abundance	[56]
	Human	mRNA (RT-qPCR, TaqMan)	Cardiac mRNA levels, A > V	[10]

<div align="center">**Table 2.** *Cont.*</div>

K$_{2P}$ Channel Subunit	Species	Protein /mRNA	Observation	Citation
	Human	mRNA (Affymetrix chip and RT-qPCR, TaqMan)	Cardiac mRNA levels, A > V mRNA abundance in Purkinje fibers	[14]
	Human	mRNA (RT-qPCR) and protein (WB)	Very low cardiac mRNA levelsDetectable protein levels	[38]
	Mouse	mRNA (RT-qPCR, TaqMan)	Moderate cardiac mRNA abundance, A and V	[16]
	Mouse	mRNA (RT-qPCR) and protein (WB)	Low cardiac mRNA abundance, A and V Cardiac protein expression	[26]
	Rat	mRNA (RT-PCR)	Cardiac mRNA abundance Cardiac mRNA adult heart > fetal heart Highest mRNA abundance in right atrium	[18]
$K_{2P}6.1$ (TWIK-2)	Rat	mRNA (RT-PCR)	Cardiac mRNA abundance	[62]
	Rat	mRNA (RT-PCR)	Moderate cardiac mRNA abundance	[15]
	Rat	mRNA (RT-qPCR, TaqMan)	Cardiac mRNA abundance in sinoatrial tissue	[19]
	Human	mRNA (NB)	No cardiac mRNA abundance	[17]
	Human	mRNA (Hybridization array)	Cardiac mRNA levels, V > A	[62]
	Human	mRNA (RT-qPCR)	mRNA abundance in human ventricular tissue mRNA abundance in iPS-derived cardiomyocytes	[22]
	Human	mRNA (RT-qPCR, TaqMan)	Low cardiac mRNA abundance	[23]
	Human	mRNA (RT-qPCR, TaqMan)	Cardiac mRNA levels, V > A	[10]
	Mouse	mRNA (RT-qPCR, TaqMan)	No cardiac mRNA abundance detectable	[16]
$K_{2P}7.1$ (TWIK-3)	Human	mRNA (RT-qPCR)	Cardiac mRNA abundance	[63]
	Human	mRNA (RT-qPCR, TaqMan)	Cardiac mRNA abundance	[23]
	Human	mRNA (RT-qPCR, TaqMan)	Very low cardiac mRNA levels, A > V	[10]
	Mouse	mRNA (RT-qPCR, TaqMan)	No cardiac mRNA abundance detectable	[16]
	Mouse	mRNA (RT-qPCR)	Low cardiac mRNA abundance	[26]
	Mouse	mRNA (RT-PCR)	Low cardiac mRNA abundance	[25]
$K_{2P}9.1$ (TASK-3)	Rat	mRNA (RT-PCR)	Low cardiac mRNA abundance, A and V	[18]
	Rat	mRNA (RT-PCR)	Cardiac mRNA abundance	[48]
	Rat	mRNA (RT-PCR)	Cardiac mRNA abundance, cardiomyocyte mRNA expression	[15]
	Rat, guinea pig, human	mRNA (RT-qPCR, TaqMan)	Human: very low cardiac mRNA abundance Rat: no cardiac mRNA abundance Guinea pig: low cardiac mRNA abundance, V > A	[49]
	Guinea pig	mRNA (RT-PCR)	No cardiac mRNA abundance	[64]

Table 2. *Cont.*

K$_{2P}$ Channel Subunit	Species	Protein /mRNA	Observation	Citation
	Human	mRNA (RT-qPCR)	Moderate mRNA abundance in human ventricular tissue mRNA abundance in iPS-derived cardiomyocytes	[22]
	Human	mRNA (RT-qPCR, TaqMan)	Very low cardiac mRNA levels, A > V	[10]
	Human	mRNA (RT-qPCR, TaqMan)	Cardiac mRNA abundance	[23]
	Human	mRNA (RT-qPCR) an protein (IF)	Strong cardiac mRNA and protein expression	[56]
K$_{2P}$10.1 (TREK-2)	Mouse	mRNA (RT-qPCR, TaqMan)	No cardiac mRNA abundance detectable	[16]
	Rat	mRNA (RT-PCR)	Cardiac mRNA levels, A > V	[18]
	Rat	mRNA (RT-PCR)	Moderate cardiac abundance	[15]
	Rat	mRNA (RT-PCR, NB)	No cardiac mRNA abundance	[65]
	Human	mRNA (RT-qPCR)	mRNA abundance in human ventricular tissue mRNA abundance in iPS-derived cardiomyocytes	[22]
	Human	mRNA (RT-qPCR, TaqMan)	Mild cardiac mRNA abundance, A > V	[41]
	Human	mRNA (RT-qPCR, TaqMan)	Low cardiac mRNA abundance	[23]
	Human	mRNA (RT-qPCR, TaqMan)	Low cardiac mRNA levels, A > V	[10]
K$_{2P}$12.1 (THIK-2)	Mouse	mRNA (RT-PCR)	Very low cardiac mRNA abundance	[15]
	Mouse	mRNA (RT-qPCR, TaqMan)	No cardiac mRNA levels detectable	[16]
	Rat	mRNA (RT-PCR)	No cardiac mRNA abundance	[66]
	Human	mRNA (NB)	Cardiac mRNA abundance	[67]
	Human	mRNA (RT-qPCR, TaqMan)	Very low cardiac mRNA abundance, A and V	[10]
K$_{2P}$13.1 (THIK-1)	Zebrafish	mRNA (RT-PCR)	Cardiac mRNA abundance	[68]
	Mouse	mRNA (RT-PCR)	Cardiac mRNA abundance	[15]
	Mouse	mRNA (RT-qPCR)	Cardiac mRNA abundance	[26]
	Mouse	mRNA (RT-qPCR, TaqMan)	Very low cardiac mRNA abundance	[16]
	Rat	mRNA (RT-PCR)	Cardiac mRNA abundance	[66]
	Human	mRNA (RT-qPCR)	mRNA abundance in human ventricular tissue mRNA abundance in iPS-derived cardiomyocytes	[22]
	Human	mRNA (RT-qPCR, TaqMan)	Low cardiac mRNA abundance	[23]
	Human	mRNA (RT-qPCR, TaqMan)	Low cardiac mRNA abundance, A > V	[10]
K$_{2P}$15.1 (TASK-5)	Mouse	mRNA (RT-qPCR)	Cardiac mRNA abundance	[26]
	Mouse	mRNA (RT-qPCR, TaqMan)	Very low cardiac mRNA abundance	[16]
	Rat	mRNA (RT-PCR)	No cardiac mRNA abundance	[48]

Table 2. *Cont.*

K$_{2P}$ Channel Subunit	Species	Protein /mRNA	Observation	Citation
	Rat	mRNA (RT-PCR)	Moderate cardiac abundance	[15]
	Human	mRNA (RT-PCR)	Cardiac mRNA abundance	[69]
	Human	mRNA (RT-PCR, NB)	No cardiac mRNA abundance	[70]
	Human	mRNA (RT-qPCR, TaqMan)	Low cardiac mRNA abundance, A and V	[10]
K$_{2P}$16.1 (TALK-1)	Rat	mRNA (NB)	No cardiac mRNA abundance	[60]
	Rat	mRNA (RT-PCR)	Moderate cardiac abundance	[15]
	Human	mRNA (NB)	No cardiac mRNA abundance	[67]
	Human	mRNA (RT-PCR, NB)	No cardiac mRNA abundance	[71]
	Human	mRNA (RT-qPCR, TaqMan)	Very low cardiac mRNA abundance, A and V	[10]
K$_{2P}$17.1 (TALK-2)	Zebrafish	mRNA (RT-PCR)	No cardiac abundance	[72]
	Rat	mRNA (NB)	Cardiac mRNA abundance	[60]
	Human	mRNA (NB)	Cardiac mRNA abundance	[67]
	Human	mRNA (RT-PCR)	Cardiac mRNA levels, A > V	[73]
	Human	mRNA (RT-qPCR)	mRNA abundance in human ventricular tissue mRNA abundance in iPS-derived cardiomyocytes	[22]
	Human	mRNA (RT-qPCR)	Cardiac mRNA abundance	[56]
	Human	mRNA (RT-qPCR)	Cardiac mRNA abundance mRNA abundance in sinoatrial and atrioventricular node Purkinje fibers > A > V	[5]
	Human	mRNA (single cell RT-qPCR) and protein (IF)	mRNA and protein abundance in iPS-derived cardiomyocytes	[74]
	Human	mRNA (RT-qPCR, TaqMan)	Cardiac mRNA levels, A > V	[10]
	Human	mRNA (RT-qPCR, TaqMan) and protein (WB)	Cardiac mRNA and protein expression	[40]
	Human	Protein (WB)	Cardiac protein expression, A	[75]
K$_{2P}$18.1 (TRESK)	Zebrafish	mRNA (ISH)	No cardiac abundance	[76]
	Mouse	mRNA (RT-qPCR, TaqMan)	Very low cardiac mRNA abundance	[77]
	Mouse	mRNA (RT-qPCR, TaqMan)	Very low cardiac mRNA abundance	[16]
	Human	mRNA (RT-PCR)	No cardiac mRNA abundance	[61]
	Human	mRNA (RT-PCR)	No cardiac mRNA abundance	[78]
	Human	mRNA (RT-qPCR, TaqMan)	Very low cardiac mRNA abundance	[10]

A, expression in atrial tissue; IF, immunofluorescence; iPS, induced pluripotent stem cell; ISH, in situ hybridization; LA, left atrium; NB, Northern blot; RT-PCR, reverse transcriptase PCR; RT-qPCR, reverse transcriptase quantitative PCR; RA, right atrium; TAC, transverse aortic constriction; TaqMan, reverse transcriptase quantitative PCR employing TaqMan® hydrolyse probes to increase specificity; V, expression in ventricular tissue; WB, Western blot.

The zebrafish possess two orthologues of the human *KCNK1* gene, *kcnk1a* and *kcnk1b* which, most likely as the result of an ancient genome duplication, both encode functional TWIK-1 channels. Knockdown of *kcnk1a* or *kcnk1b* in zebrafish embryos resulted in a phenotype atrial dilatation and bradycardia, suggesting a role of $K_{2P}1.1$ (TWIK-1) in regulation of sinus node function and structural heart development [11]. Further, downregulation of cardiac *Kcnk1* mRNA levels was reported in a diabetic rat model, displaying again a phenotype of sinus bradycardia [19]. The presence of single nucleotide polymorphisms in the *KCNK1* gene might be correlated with the prevalence of coronary artery disease [79]. Christensen et al. reported the identification of three non-synonymous *KCNK1* gene variants (p.R171H, p.I98M, and p.G236S) in a cohort of 373 atrial fibrillation (AF) patients. Although these variants are localized in highly conserved domains, no effect on potassium current, reversal potential, or subcellular localization was detected in heterologous expression systems [11]. Pharmacological modulation of homodimeric $K_{2P}1.1$ (TWIK-1) channels by quinine and quinidine was described (Table 3) [20]. In our own studies, AF and heart failure patients showed unchanged cardiac *KCNK1* mRNA levels [10,40], while others reported upregulation of *KCNK1* mRNA patients with atrial dilatation [11] or Brugada syndrome [80], downregulation of *KCNK1* mRNA in AF [12] or mitral valve disease [81].

Table 3. Pharmacological profile of K_{2P}-channels.

K_{2P} Channel	Drug/Compound	Effect (Organism)	EC_{50} /IC_{50} (Organism)	Citation
$K_{2P}1.1$ (TWIK-1)	Quinine	Inhibition (XO)	50 μM (XO)	[20]
	Quinidine	Inhibition (XO)	95 μM (XO)	[20]
	Barium	Inhibition (XO)	100 μM (XO)	[20]
	Charybdotoxin	< 10% inhibition at 3 nM (XO)	n.m.	[20]
	Dendrotoxin	< 10% inhibition at 100 nM (XO)	n.m.	[20]
	Apamin	< 10% inhibition at 300 nM (XO)	n.m.	[20]
	Clofilium	< 10% inhibition at 30 μM (XO)	n.m.	[20]
	Glibenclamid	< 10% inhibition at 30 μM (XO)	n.m.	[20]
	Cromakalim	No effect at 100 μM (XO)	n.m.	[20]
	Tedisamil	30% inhibition at 100 μM (XO)	n.m.	[20]
	Dronedarone	No significant effect at 100 μM (XO)	n.m.	[82]
	Amiodarone	< 10% inhibition at 100 μM (XO)	n.m.	[20]
	Pinacidil	No effect at 100 μM (XO)	n.m.	[20]
	Vernakalant	No significant effect at 100 μM (XO)	n.m.	[83]
	Flecainide	No significant effect at 100 μM (XO)	n.m.	[84]
	Genistein	No significant effect at 100 μM (XO)	n.m.	[85]
	4-AP	< 10% inhibition at 1 mM (XO)	n.m.	[20]
	TEA	30% inhibition at 10 mM (XO)	n.m.	[20]
$K_{2P}2.1$ (TREK-1)	**GI-530159**	**High affinity $K_{2P}2.1$ activator (MC)**	**890 nM (MC)**	[86]
	Copper	Activation (MC)	3 μM (MC)	[87]
	Ostruthin	Activator (MC)	5.3 μM (MC)	[88]
	BL-1249	**High affinity TREK-1/2 activator (XO)**	**5.5 μM (XO)**	[89]
	ML402	**High affinity TREK-1/2 activator (XO)**	**13.7 μM (XO)**	[90]
	ML335	**High affinity TREK-1/2 activator (XO)**	**14.3 μM (XO)**	[90]
	ML67-33	**High affinity TREK-1/2 activator (XO)**	**36.3 μM (XO); 9.7 μM (MC)**	[91]
	Pranlukast	66.4% activation at 3 μM (MC)	n.m.	[92]
	DCPIB	~3-fold activation at 10 μM (MC)	n.m.	[93]

Table 3. *Cont.*

K$_{2P}$ Channel	Drug/Compound	Effect (Organism)	EC$_{50}$/IC$_{50}$ (Organism)	Citation
	Morphine	~2-fold activation at 10 μM (MC)	n.m.	[94]
	Flufenamic acid	~4-fold activation at 100 μM (MC)	n.m.	[95]
	Niflumic acid	~2.5-fold activation at 100 μM (MC)	n.m.	[95]
	Mefenamic acid	~2-fold activation at 100 μM (MC)	n.m.	[95]
	Carbamazepine	42% activation at 100 μM (MC)	n.m.	[96]
	Valproate	28% activation at 100 μM (MC)	n.m.	[96]
	Gabapentin	25% activation at 100 μM (MC)	n.m.	[96]
	Diethyl ether	~1.75-fold activation at 600 μM (MC)	n.m.	[97]
	Chloroform	~3.5-fold activation at 800 μM (MC)	n.m.	[97]
	Lithium	31% activation at 1 mM (MC)	n.m.	[96]
	Rubidium	27% activation at 1 mM (MC)	n.m.	[96]
	Halothane	~1.4-fold activation at 1 mM (MC)	n.m.	[97]
	Isoflurane	~1.5-fold activation at 2 mM (MC)	n.m.	[97]
	Cyclopropane	~30% activation at 10% (MC)	n.m.	[98]
	Xenon	~30% activation at 80% (MC)	n.m.	[98]
	Nitrous oxide	~30% activation at 80% (MC)	n.m.	[98]
	Spadin	**High affinity K$_{2P}$2.1 inhibitor (MC)**	**40 nM (MC)**	**[99]**
	Amlodipin	Inhibition (MC)	430 nM (MC)	[100]
	Nigludipine	Inhibition (MC)	750 nM (MC)	[100]
	Pimozide	Inhibition (MC)	1.8 μM (MC)	[101]
	Fluphenthixol	Inhibition (MC)	2.0 μM (MC)	[101]
	Chlorpromazine	Inhibition (MC)	2.7 μM (MC)	[96,101]
	Sipatrigine	73.3% inhibition at 10 μM (MC)	4 μM	[59]
	Fluphenazine	Inhibition (MC)	4.7 μM (MC)	[101]
	Haloperidol	Inhibition (MC)	5.5 μM (MC)	[101]
	Norfluoxetine	Inhibition (MC)	9 μM (MC)	[102]
	Vernakalant	Inhibition (MC)	13.3 μM (MC)	[84]
	Loxapine	Inhibition (MC)	19.7 μM (MC)	[101]
	Fluoxetine	Inhibition (MC)	19–37.9 μM (MC)	[96,102]
	Carvedilol	Inhibition (XO, MC)	20.3 μM (XO); 1.6 μM (MC)	[42]
	A1899 (*High affinity K$_{2P}$3.1 inhibitor*)	Inhibition (XO)	23.8 μM (XO)	[103]
	Dronedarone	Inhibition (XO, MC)	26.7 μM (XO); 6.1 μM (MC)	[82]
	Propafenone	Inhibition (XO, MC)	51.0 μM (XO); 7.9 μM (MC)	[104]
	Levobupivacaine	Inhibition (MC)	126 μM (MC)	[105]
	Diltiazem	Inhibitor (MC)	180 μM (MC)	[95]
	Lidocaine	Inhibition (MC)	207 μM (MC)	[106]
	Bupivacaine	Inhibition (MC)	370 μM (MC)	[107]
	Caffeine	Inhibition (MC)	377 μM (MC)	[108]
	Ropivacaine	Inhibition (MC)	402 μM (MC)	[105]
	Theophylline	Inhibition (MC)	486 μM (MC)	[108]
	Zinc	Inhibition (MC)	659 μM (MC)	[87]
	Mexiletine	Inhibition (XO, MC)	1.3 mM (XO); 182 μM (MC);	[104]
	Tetramethyl-ammonium	63% inhibition (MC)	n.m.	[24]
	Lamotrigine	~10% inhibition at 10 μM (MC)	n.m.	[59]

Table 3. *Cont.*

K$_{2P}$ Channel	Drug/Compound	Effect (Organism)	EC$_{50}$ /IC$_{50}$ (Organism)	Citation
	Metoprolol	~20% inhibition at 100 μM (XO)	n.m.	[42]
	Propranolol	~30% inhibition at 100 μM (XO)	n.m.	[42]
	Citalopram	59% inhibition at 100 μM (MC)	n.m.	[96]
	Barium	50% inhibition at 300 μM (XO)	n.m.	[24]
	Ranolazine	7.35% inhibition at 300 μM (XO)	n.m.	[109]
	Clozapine	Inhibition (MC)	n.m.	[101]
	Sulpiride	No significant effect at 10 μM (MC)	n.m.	[101]
	Tiapride	No significant effect at 10 μM (MC)	n.m.	[101]
	Glibenclamide	No significant effect at 10 μM (XO)	n.m.	[24]
	Cesium	No significant effect at 100 μM (XO)	n.m.	[24]
	Gadolineum	No significant effect at 100 μM (XO)	n.m.	[24]
	TEA	No significant effect at 100 μM (XO)	n.m.	[24]
	Quinine	No significant effect at 100 μM (XO)	n.m.	[24]
	Quinidine	No significant effect at 100 μM (XO)	n.m.	[24]
	Tedisamil	No significant effect at 100 μM (XO)	n.m.	[24]
	Genistein	No significant effect at 100 μM (XO)	n.m.	[85]
	Flecainide	No significant effect at 100 μM (XO, MC)	n.m.	[84]
	Amiodarone	No significant effect (XO)	n.m.	[110]
	Sotalol	No significant effect (XO)	n.m.	[82]
	Digoxin	No significant effect (XO)	n.m.	[111]
	Digitoxin	No significant effect (XO)	n.m.	[111]
	A293	No significant effect (XO)	n.m.	[10]
	Ajmaline	No significant effect (MC)	n.m.	[104]
	GsMTx4	No significant effect (MC)	n.m.	[112]
	Magnesium	No significant effect (XO)	n.m.	[24]
	Halothane	Activation (XO, MC)	300–1000 μM (XO)	[97,113,114]
	Sevoflurane	~40% activation at 1 mM	n.m.	[114]
	Isoflurane	~15% activation at 1 mM (XO) ~20% activation at 2 mM (MC)	n.m.	[97,113]
	BAY2341237	**High affinity K$_{2P}$3.1 inhibitor**	**7.6 nM (XO)**	[115]
	BAY1000493	**High affinity K$_{2P}$3.1 inhibitor**	**9.5 nM (XO)**	[115]
	ML365	**High affinity K$_{2P}$3.1 inhibitor**	**16 nM (MC)**	[116]
	A1899 (S20951)	**High affinity K$_{2P}$3.1 inhibitor**	**35 nM (XO); 7 nM (MC)**	[103,115]
K$_{2P}$3.1 (TASK-1)	S9947 (K$_V$1.5 blocker)	Inhibition (XO)	200 nM (XO)	[103,117]
	A293 (AVE1231)	**High affinity K$_{2P}$3.1 inhibitor**	**222 nM (XO)**	[10,15]
	PK-THPP	Inhibition (XO)	243 nM	[118]
	MSD-D (K$_V$1.5 blocker)	Inhibition (XO)	350 nM (XO)	[117]
	Amiodarone	Inhibition (XO)	400 nM (XO)	[82,110]
	Doxapram	Inhibition (XO, MC)	410 nM (XO)	[119]
	AVE0118 (K$_V$1.5 blocker)	Inhibition (XO)	600 nM (XO)	[117]
	Methanandamide	Inhibition (XO)	700 nM (MC)	[120]
	Digoxin	Inhibition (XO)	900 nM (XO)	[111]

Table 3. *Cont.*

K$_{2P}$ Channel	Drug/Compound	Effect (Organism)	EC$_{50}$ /IC$_{50}$ (Organism)	Citation
	ICAGEN-4 (*K$_V$1.5 blocker*)	Inhibition (XO)	1.05 μM (XO)	[117]
	ML308 (*High affinity K$_{2P}$9.1 inhibitor*)	Inhibition (MC)	3.2 μM (MC)	[121]
	Carvedilol	Inhibition (XO, MC)	3.8 μM (XO); 0.83 μM (MC)	[42]
	Digitoxin	Inhibition (XO)	7.4 μM (XO)	[111]
	Genistein	81.1% inhibition at 100 μM (XO)	12.3 μM (MC)	[85]
	Dronedarone	Inhibition (XO, MC)	18.7 μM (XO); 5.2 μM (MC)	[82]
	Propafenone	Inhibition (XO, MC)	18.1 μM (XO); 5.1 μM (MC);	[104]
	Etidocaine	Inhibition (XO)	39 μM (XO)	[122]
	Ostruthin	Inhibition (MC)	41 μM (MC)	[88]
	R-Ropivacaine	Inhibition (XO)	51 μM (XO)	[122]
	S-Ropivacaine	Inhibition (XO)	53 μM (XO)	[122]
	Bupivacaine	Inhibition (XO)	68 μM (XO)	[123]
	Etomidate	Inhibition (XO)	119 μM (XO)	[113]
	Zinc	Inhibition (XO)	175 μM (XO)	[123]
	Ranolazine	Inhibition (XO, MC)	198.4 μM (XO); 30.6 μM (MC)	[109]
	Lidocain	Inhibition (XO)	222 μM (XO)	[122]
	Mexiletine	Inhibition (XO, MC)	405 μM (XO); 97.3 μM (MC)	[104]
	Tetracaine	Inhibition (XO)	668 μM	[122]
	Mepivacaine	Inhibition (XO)	709 μM (XO)	[122]
	Agitoxin	< 15%inhibition at 1 nM (XO)	n.m.	[123]
	Margatoxin	< 15%inhibition at 10 nM (XO)	n.m.	[123]
	Dendrotoxin	< 15%inhibition at 100 nM (XO)	n.m.	[123]
	Charybdotoxin	< 15%inhibition at 200 nM (XO)	n.m.	[123]
	Anandamide	~90% inhibition at 3 μM (MC)	n.m.	[120]
	CP55940 (*CB1/CB2agonist*)	~50% inhibition at 10 μM (MC)	n.m.	[120]
	Sipatrigine	37%inhibition at 10 μM (MC)	n.m.	[59]
	Glibenclamid	< 15%inhibition at 30 μM (XO)	n.m.	[123]
	Propranolol	~60% inhibition at 100 μM (XO)	n.m.	[42]
	Cesium	31% inhibition at 100 μM (XO)	n.m.	[45]
	Quinidine	< 20–71 % inhibition at 100 μM (XO)	n.m.	[45,123]
	Quinine	< 20 % inhibition at 100 μM (XO)	n.m.	[45]
	Quinacrine	< 20% inhibition at 100 μM (XO)	n.m.	[45]
	Barium	~19% inhibition at 100 μM (XO)	n.m.	[45]
	Daidzein	18.2% inhibition at 100 μM (XO)	n.m.	[85]
	Cromakalim	< 15%inhibition at 100 μM (XO)	n.m.	[123]
	Metoprolol	~10% inhibition at 100 μM (XO)	n.m.	[42]
	Phenytoin	~50% inhibition at 200 μM (XO)	n.m.	[123]
	Diethyl ether	~45 % at 600 μM (MC)	n.m.	[97]
	Magnesium	~14% inhibition at 10 mM (XO)	n.m.	[123]
	4-AP	<15%inhibition at 10 mM (XO)	n.m.	[45,123]
	Flecainide	No significant effect at 100 μM (XO, MC)	n.m.	[84]
	Ouabain	No significant effect at 100 μM (XO)	n.m.	[111]

Table 3. *Cont.*

K$_{2P}$ Channel	Drug/Compound	Effect (Organism)	EC$_{50}$/IC$_{50}$ (Organism)	Citation
	Vernakalant	No significant effect at 100 μM (XO, MC)	n.m.	[84]
	Sotalol	No significant effect at 100 μM (XO)	n.m.	[82]
	Genistin	No significant effect at 100 μM (XO)	n.m.	[85]
	Propofol	No significant effect at 200 μM (XO)	n.m.	[113]
	Chloroform	No significant effect at 800 μM (MC)	n.m.	[97]
	TEA	No significant effect at 1 mM (XO)	n.m.	[45]
	Sipatrigine	45%inhibition at 10 μM (MC)	10 μM	[59]
	ML67-33 *(High affinity TREK-1/2 activator)*	Activation (XO, MC)	27.3 μM (XO); 1.8 μM (MC)	[91]
	BL-1249 *(High affinity TREK-1/2 activator)*	Activation (XO)	48 μM (XO)	[89]
	A1899 *(High affinity K$_{2P}$3.1 inhibitor)*	Inhibition (XO)	>20 μM (XO)	[103]
	Docosahexaenoate	~12-fold activation at 10 μM (MC)	n.m.	[58]
	Eicosapentaenoate	~8-fold activation at 10 μM (MC)	n.m.	[58]
	Arachidonic acid	~5-fold activation at 10 μM (MC)	n.m.	[58]
	Oleate	~1.5-fold activation at 10 μM (MC)	n.m.	[58]
	Linoleate	~1.5-fold activation at 10 μM (MC)	n.m.	[58]
	Riluzole	3.9-fold activation at 100 μM (MC)	n.m.	[58]
	Flufenamic acid	~2-fold activation at 100 μM (MC)	n.m.	[95]
	Niflumic acid	~2-fold activation at 100 μM (MC)	n.m.	[95]
	Mefenamic acid	~1.6-fold activation at 100 μM (MC)	n.m.	[95]
	Lamotrigine	~10% inhibition at 10 μM (MC)	n.m.	[59]
K$_{2P}$4.1 (TRAAK)	Vernakalant	17.1% inhibition at 100 μM (XO)	n.m.	[83]
	Barium	56.7% inhibition at 1 mM (XO)	n.m.	[58]
	Charybdotoxin	No significant effect at 20 nM (XO)	n.m.	[58]
	Dendrotoxin	No significant effect at 100 nM (XO)	n.m.	[58]
	Tetrodotoxin	No significant effect at 1 μM (XO)	n.m.	[58]
	Tedisamil	No significant effect at 10 μM (XO)	n.m.	[58]
	Palmitate	No significant effect at 10 μM (MC)	n.m.	[58]
	Stearate	No significant effect at 10 μM (MC)	n.m.	[58]
	Arachidate	No significant effect at 10 μM (MC)	n.m.	[58]
	Fluphenazine	No significant effect at 10 μM (MC)	n.m.	[101]
	Chlorpromazine	No significant effect at 10 μM (MC)	n.m.	[101]
	Haloperidol	No significant effect at 10 μM (MC)	n.m.	[101]
	Fluphenthixol	No significant effect at 10 μM (MC)	n.m.	[101]
	Loxapine	No significant effect at 10 μM (MC)	n.m.	[101]
	Pimozide	No significant effect at 10 μM (MC)	n.m.	[101]
	Clozapine	No significant effect at 10 μM (MC)	n.m.	[101]
	Sulpiride	No significant effect at 10 μM (MC)	n.m.	[101]
	Tiapride	No significant effect at 10 μM (MC)	n.m.	[101]
	Tolbutamide	No significant effect at 100 μM (XO)	n.m.	[58]
	Pinacidil	No significant effect at 100 μM (XO)	n.m.	[58]
	P1060	No significant effect at 100 μM (XO)	n.m.	[58]

Table 3. *Cont.*

K$_{2P}$ Channel	Drug/Compound	Effect (Organism)	EC$_{50}$ /IC$_{50}$ (Organism)	Citation
	Glibenclamide	No significant effect at 200 μM (XO)	n.m.	[58]
	Cobalt	No significant effect at 500 μM (XO)	n.m.	[58]
	Dronedarone	No significant effect at 100 μM (XO)	n.m.	[82]
	Flecainide	No significant effect at 100 μM (XO)	n.m.	[84]
	Genistein	No significant effect at 100 μM (XO)	n.m.	[85]
	Ranolazine	3.32 % inhibition at 300 μM (XO)	n.m.	[109]
	Diethyl ether	No significant effect at 600 μM (MC)	n.m.	[97]
	Chloroform	No significant effect at 800 μM (MC)	n.m.	[97]
	Halothane	No significant effect at 1 mM (MC)	n.m.	[97]
	Diltiazem	No significant effect at 1 mM (MC)	n.m.	[95]
	TEA	No significant effect at 1 mM (XO)	n.m.	[58]
	4-AP	No significant effect at 1 mM (XO)	n.m.	[58]
	Caesium	No significant effect at 1 mM (XO)	n.m.	[58]
	Isoflurane	No significant effect at 2 mM (MC)	n.m.	[97]
	Digoxin	No significant effect (XO)	n.m.	[111]
	Digitoxin	No significant effect (XO)	n.m.	[111]
	A293 *(High affinity K$_{2P}$3.1 inhibitor)*	Inhibition (XO)	8.1 nM (XO)	[10,15]
	A1899 *(High affinity K$_{2P}$3.1 inhibitor)*	Inhibition (XO)	12 μM (XO)	[103]
	Quinine	Inhibition (XO)	22.4 μM (XO)	[17]
	Quinidine	65% inhibition at 100 μM (XO)	n.m.	[17]
	Zinc	15.3% inhibition at 100 μM (XO)	n.m.	[17]
	Ranolazine	30.02% inhibition at 300 μM (XO)	n.m.	[17]
K$_{2P}$5.1 *(TASK-2)*	Barium	16.9% inhibition at 1 mM (XO)	n.m.	[17]
	Lidocaine	60.4% inhibition at 10 mM (XO)	n.m.	[17]
	Bupivacaine	80.9% inhibition at 10 mM (XO)	n.m.	[17]
	Arachidonic acid	No significant effect at 10 μM (XO)	n.m.	[17]
	4-AP	No significant effect at 100 μM (XO)	n.m.	[17]
	Dronedarone	No significant effect at 100 μM (XO)	n.m.	[82]
	Flecainide	No significant effect at 100 μM (XO)	n.m.	[84]
	Genistein	No significant effect at 100 μM (XO)	n.m.	[85]
	Vernakalant	No significant effect at 100 μM (XO)	n.m.	[83]
	Digoxin	No significant effect (XO)	n.m.	[111]
	Digitoxin	No significant effect (XO)	n.m.	[111]
	TEA	No significant effect at 1 mM (XO)	n.m.	[17]
	Cesium	No effect at 1 mM (XO)	n.m.	[17]
	Barium	Inhibition (MC)	~100 μM (MC)	[124]
	Quinidine	73% inhibition at 100 μM (XO)	n.m.	[124]
	Quinine	73% inhibition at 100 μM (XO)	n.m.	[124]
K$_{2P}$6.1 *(TWIK-2)*	Genistein	~30% inhibition at 100 μM (XO)	n.m.	[85]
	Dronedarone	10.7% inhibition at 100 μM (XO)	n.m.	[82]
	Chloroform	32% inhibition at 300 μM (XO)	n.m.	[124]
	Halothane	27% inhibition at 750 μM (XO)	n.m.	[124]

Table 3. *Cont.*

K$_{2P}$ Channel	Drug/Compound	Effect (Organism)	EC$_{50}$ /IC$_{50}$ (Organism)	Citation
	Cesium	92% inhibition of inward current at 10 mM (XO)	n.m.	[124]
	TEA	No significant effect at 5 mM (XO)	n.m.	[124]
	4-AP	No significant effect at 3 mM (XO)	n.m.	[124]
	Glibenclamide	No significant effect at 10 μM (XO)	n.m.	[124]
	Vernakalant	No significant effect at 100 μM (XO)	n.m.	[83]
	Flecainide	No significant effect at 100 μM (XO)	n.m.	[84]
K$_{2P}$7.1 *(TWIK-3)*		*Non-functional channel*		
	DCPIB	~3-fold activation at 10 μM (MC)	n.m.	[93]
	Halothane	65.6% activation at 1 mM (XO)	n.m.	[125]
	BAY2341237 *(High affinity K$_{2P}$3.1 inhibitor)*	Inhibition (XO)	2.3 nM (XO)	[115]
	BAY1000493 *(High affinity K$_{2P}$3.1 inhibitor)*	Inhibition (XO)	15.1 nM (XO)	[115]
	A1899 *(High affinity K$_{2P}$3.1 inhibitor)*	Inhibition (XO, MC)	318 nM (XO); 70 nM (MC)	[103]
	ML308	**High affinity K$_{2P}$9.1 inhibitor**	**413 nM (MC)**	**[121]**
	A293 *(High affinity K$_{2P}$3.1 inhibitor)*	Inhibition (XO)	950 nM (XO)	[10,15]
	ML365 *(High affinity K$_{2P}$3.1 inhibitor)*	Inhibition (MC)	990 nM (MC)	[116]
K$_{2P}$9.1 *(TASK-3)*	Copper	Inhibition (MC)	2.7 μM (MC)	[87]
	Zinc	Inhibition (MC)	12.7 μM (MC)	[87]
	Mibefradil	Inhibition (MC)	24.6 μM (MC)	[126]
	Doxapram	Inhibition (XO)	37 μM (XO)	[119]
	L-703,606 oxalate	Inhibition (MC)	45.5 μM (MC)	[126]
	Oligomycine A	Inhibition (MC)	47.7 μM (MC)	[126]
	GW2974	Inhibition (MC)	50.1 μM (MC)	[126]
	Loratadine	Inhibition (MC)	63.4 μM (MC)	[126]
	Dihydro-β-erythroidine hydrobromide	Inhibition (MC)	73.8 μM (MC)	[126]
	(±)-Octoclothepin maleate	Inhibition (MC)	73.8 μM (MC)	[126]
	Ruthenium red	Inhibitor (XO)	114 μM	[127]
	Etomidate	Inhibition (XO)	128 μM (XO)	[113]
	Mevastatin	Inhibition (MC)	159 μM (MC)	[126]
	Ostruthin	Inhibition (MC)	227 μM (MC)	[88]
	Barium	11% inhibition at 100 μM (XO)	290 μM (XO)	[64]
	Arachidonic acid	4.81% inhibition at 10 μM (XO)	n.m.	[125]
	Genistein	~60% inhibition at 100 μM (XO)	n.m.	[85]
	Bupivacaine	50.2–56% inhibition at 100 μM (XO, MC)	n.m.	[70,125]
	Alphaxolone	49.2% inhibition at 100 μM (XO)	n.m.	[125]
	Quinidine	42.2% inhibition at 100 μM (XO)	n.m.	[125]

K$_{2P}$ Channel	Drug/Compound	Effect (Organism)	EC$_{50}$ /IC$_{50}$ (Organism)	Citation
	Quinine	36.9% inhibition at 100 μM (XO)	n.m.	[125]
	Dronedarone	31.7% inhibition at 100 μM (XO)	n.m.	[82]
	Fluoxetine	31%inhibition at 100 μM (MC)	n.m.	[102]
	Ketamine	7.3% inhibition at 100 μM (XO)	n.m.	[125]
	Pentobarbital	4.3% inhibition at 100 μM (XO)	n.m.	[125]
	Glibenclamide	3.6% inhibition at 100 μM (XO)	n.m.	[125]
	Ranolazine	28.28% inhibition at 300 μM (XO)	n.m.	[109]
	TEA	6% inhibition at 1 mM (XO)	n.m.	[125]
	Xenon	No significant effect at 80% (MC)	n.m.	[98]
	Nitrous oxide	No significant effect at 80% (MC)	n.m.	[98]
	Cyclopropane	No significant effect at 10% (MC)	n.m.	[98]
	Propofol	No significant effect at 200 μM (XO)	n.m.	[113]
	Vernakalant	No significant effect at 100 μM (XO)	n.m.	[83]
	Flecainide	No significant effect at 100 μM (XO)	n.m.	[84]
	Digoxin	No significant effect (XO)	n.m.	[111]
	Digitoxin	No significant effect (XO)	n.m.	[111]
	Cesium	8–12% inhibition at 10 mM (XO)	n.m.	[64,125]
	Ostruthin	Activator (MC)	3.7 μM (MC)	[88]
	ML335	**High affinity TREK-1/2 activator**	**5.2 μM (XO)**	[90]
	ML402	**High affinity TREK-1/2 activator**	**5.9 μM (XO)**	[90]
	Arachidonic acid	Activation (MC)	7.3 μM (MC)	[65]
	BL-1249	**High affinity TREK-1/2 activator**	**8.0 μM (XO)**	[89]
	ML67-33	**High affinity TREK-1/2 activator**	**30.2 μM (XO); 1.6 μM (MC)**	[91]
	11-deoxyprostaglandin F2α	~5-fold activation at 2 μM (MC)	n.m.	[128]
	Pranlukast	228 % activation at 3 μM (MC)	n.m.	[92]
	Ocosahexaenoicacid	~5-fold activation at 20 μM (MC)	n.m.	[65]
	Linolenic acid	~6-fold activation at 20 μM (MC)	n.m.	[65]
	Eicosapentaenoic acid	~8-fold activation at 20 μM (MC)	n.m.	[65]
	Linoleic acid	~8-fold activation at 20 μM (MC)	n.m.	[65]
	Flufenamic acid	~4-fold activation at 100 μM (MC)	n.m.	[95]
K$_{2P}$10.1 (TREK-2)	Niflumic acid	~2.5-fold activation at 100 μM (MC)	n.m.	[95]
	Mefenamic acid	~2-fold activation at 100 μM (MC)	n.m.	[95]
	Ruthenium red	Inhibition (XO)	230 nM (XO)	[127]
	A1899 (High affinity K$_{2P}$3.1 inhibitor)	Inhibition (XO)	8.4 μM (XO)	[103]
	Carvedilol	Inhibition (XO, MC)	24 μM (XO); 7.6 (MC)	[43]
	Fluoxetine	68% inhibition at 10 μM (MC)	28.7 μM (MC)	[96]
	Diltiazem	Inhibition (MC)	330 μM (MC)	[95]
	Fluphenthixol	~80% inhibition at 10 μM (MC)	n.m.	[101]
	Pimozide	~80% inhibition at 10 μM (MC)	n.m.	[101]
	Fluphenazine	~70% inhibition at 10 μM (MC)	n.m.	[101]
	Clozapine	~50% inhibition at 10 μM (MC)	n.m.	[101]
	Loxapine	~50% inhibition at 10 μM (MC)	n.m.	[101]

Table 3. *Cont.*

K$_{2P}$ Channel	Drug/Compound	Effect (Organism)	EC$_{50}$ /IC$_{50}$ (Organism)	Citation
	Haloperidol	~50% inhibition at 10 μM (MC)	n.m.	[101]
	Paroxetin	33% inhibition at 20 μM (MC)	n.m.	[96]
	Citalopram	59% inhibition at 100 μM (MC)	n.m.	[96]
	Chlorpromazine	57% inhibition at 100 μM (MC)	n.m.	[96,101]
	Vernakalant	19.8% inhibition at 100 μM (XO)	n.m.	[83]
	Barium	36% inhibition at 2 mM (MC)	n.m.	[65]
	Sulpiride	No significant effect at 10 μM (MC)	n.m.	[101]
	Tiapride	No significant effect at 10 μM (MC)	n.m.	[101]
	Elaidic acid	No significant effect at 20 μM (MC)	n.m.	[65]
	Stearic acid	No significant effect at 100 μM (MC)	n.m.	[65]
	Palmitic acid	No significant effect at 100 μM (MC)	n.m.	[65]
	Gabapentin	No significant effect at 100 μM (MC)	n.m.	[96]
	Valproate	No significant effect at 100 μM (MC)	n.m.	[96]
	Carbamazepine	No significant effect at 100 μM (MC)	n.m.	[96]
	Flecainide	No significant effect at 100 μM (XO)	n.m.	[84]
	Genistein	No significant effect at 100 μM (XO)	n.m.	[85]
	Dronedarone	No significant effect at 100 μM (XO)	n.m.	[82]
	Quinidine	No significant effect at 100 μM (MC)	n.m.	[65]
	Bupivacaine	No significant effect at 100 μM (MC)	n.m.	[65]
	Gadolinium	No significant effect at 100 μM (MC)	n.m.	[65]
	Ranolazine	No significant effect at 300 μM (XO)	n.m.	[109]
	TEA	No significant effect at 1 mM (MC)	n.m.	[65]
	Lidocaine	No significant effect at 1 mM (MC)	n.m.	[65]
	Lithium	No significant effect at 1 mM (MC)	n.m.	[96]
	Rubidium	No significant effect at 1 mM (MC)	n.m.	[96]
	Digitoxin	No significant effect (XO)	n.m.	[111]
	Digoxin	No significant effect (XO)	n.m.	[111]
K$_{2P}$12.1	Quinidine	Inhibition (XO)	160 μM (XO)	[8]
	Halothane	~50% inhibition at 5 mM (XO)	n.m.	[8]
	Arachidonic acid	No significant effect at 5 μM (XO)	n.m.	[8]
K$_{2P}$13.1 (THIK-1)	Lysophos-phatidylcholine	~20% activation at 10 μM (XO)	n.m.	[66]
	Arachidonic acid	69.6–85% activation at 5–20 μM (XO)	980 nM (XO)	[66,68]
	Dronedarone	14.9% activation at 100 μM (XO)	n.m.	[82]
	Quinidine	10.9% activation at 100 μM (XO)	n.m.	[129]
	Amiodarone	9.3% activation at 100 μM	n.m.	[129]
	Ranolazine	4.98% activation at 300 μM (XO)	n.m.	[109]
	A1899 (High affinity K$_{2P}$3.1 inhibitor)	Inhibition (XO)	2.2 μM (XO)	[103]
	Mexiletine	74.6% inhibition at 1.5 mM (XO)	356 μM (XO)	[68,129]
	Halothane	56% inhibition at 5 mM (XO)	2.8 mM (XO)	[66]
	Lidocaine	59.2% inhibition at 100 μM (XO)	n.m.	[68]
	Carvedilol	No significant effect at 100 μM (XO)	n.m.	[129]
	Metoprolol	No significant effect at 100 μM (XO)	n.m.	[129]
	Vernakalant	No significant effect at 100 μM (XO)	n.m.	[83]
	Flecainide	No significant effect at 100 μM (XO)	n.m.	[84]

<div align="center">**Table 3.** *Cont.*</div>

K$_{2P}$ Channel	Drug/Compound	Effect (Organism)	EC$_{50}$ /IC$_{50}$ (Organism)	Citation
	Verapamil	No significant effect at 100 μM (XO)	n.m.	[129]
	Propafenone	26% inhibition at 100 μM (XO)	n.m.	[129]
	Genistein	~20% inhibition at 100 μM (XO)	n.m.	[85]
	Propranolol	37.6% inhibition at 200 μM (XO)	n.m.	[129]
	Chloroform	No significant effect at 1 mM (XO)	n.m.	[66]
	Barium	88.7% inhibition at 2 mM (XO)	n.m.	[66,68]
	Digoxin	No significant effect (XO)	n.m.	[111]
	Digitoxin	No significant effect (XO)	n.m.	[111]
K$_{2P}$15.1 (TASK-5)		*Non-functional channel*		
	Digitoxin	~30% inhibition at 100 μM (XO)	n.m.	[111]
	Ranolazine	23.04% inhibition at 300 μM (XO)	n.m.	[109]
	Halothane	26.8% inhibition at 800 μM (XO)	n.m.	[67]
	Chloroform	21.5% inhibition at 800 μM (XO)	n.m.	[67]
	Barium	51.4% inhibition at 1 mM (XO)	n.m.	[67]
	Quinine	45.1% inhibition at 1 mM (XO)	n.m.	[67]
	Quinidine	36.8% inhibition at 1 mM (XO)	n.m.	[67]
K$_{2P}$16.1 (THIK-1)	TEA	14.9% inhibition at 1 mM (XO)	n.m.	[67]
	Arachidonic acid	No significant effect at 20 μM (XO)	n.m.	[67]
	4-AP	No significant effect at 100 μM (XO)	n.m.	[67]
	Vernakalant	No significant effect at 100 μM (XO)	n.m.	[83]
	Flecainide	No significant effect at 100 μM (XO)	n.m.	[84]
	Genistein	No significant effect at 100 μM (XO)	n.m.	[85]
	Dronedarone	No significant effect at 100 μM (XO)	n.m.	[82]
	Isoflurane	No significant effect at 800 μM (XO)	n.m.	[67]
	Cesium	No significant effect at 1 mM (XO)	n.m.	[67]
	Digoxin	No significant effect (XO)	n.m.	[111]
	A1899 (High affinity K$_{2P}$3.1 inhibitor)	Inhibition (XO)	8.1 μM (XO)	[103]
	A293 (High affinity K$_{2P}$3.1 inhibitor)	Inhibition (XO)	18.1 μM (XO)	[10,15]
	Propafenone	296.1% activation at 100 μM (XO, MC)	75.4 μM (XO)	[75]
	Quinidine	57.7% activation at 100 μM (XO)	n.m.	[75]
	Mexiletine	20.6% activation at 100 μM (XO)	n.m.	[75]
	Verapamil	20.5% inhibition at 100 μM (XO)	n.m.	[75]
	Amiodarone	12.5% inhibition at 100 μM (XO)	n.m.	[75]
	Sotalol	9.8% inhibition at 100 μM (XO)	n.m.	[75]
K$_{2P}$17.1 (THIK-2)	Ranolazine	8.3–34.88% inhibition at 100–300 μM (XO)	n.m.	[75,109]
	Barium	81.2–82.8% inhibition at 2 mM (XO)	n.m.	[67,72,73]
	Cesium	No significant effect at 1–2 mM (XO)	n.m.	[67,73]
	Arachidonic acid	No significant effect at 100 μM (XO)	n.m.	[67,73]
	Flecainide	No significant effect at 100 μM (XO)	n.m.	[84]
	Genistein	No significant effect at 100 μM (XO)	n.m.	[85]
	Carvedilol	No significant effect at 100 μM (XO)	n.m.	[75]
	Amitriptyline	No significant effect at 100 μM (XO)	n.m.	[75]

Table 3. *Cont.*

K$_{2P}$ Channel	Drug/Compound	Effect (Organism)	EC$_{50}$ /IC$_{50}$ (Organism)	Citation
	Ajmaline	No significant effect at 100 μM (XO)	n.m.	[75]
	Vernakalant	No significant effect at 100 μM (XO)	n.m.	[83]
	Dronedarone	No significant effect at 100 μM (XO)	n.m.	[82]
	Digoxin	No significant effect (XO)	n.m.	[111]
	Digitoxin	No significant effect (XO)	n.m.	[111]
	Metoprolol	17.3% activation at 100 μM (XO)	n.m.	[75]
	Propranolol	139.2% activation at 100 μM (XO)	n.m.	[75]
	Bupivacaine	25.7% inhibition at 1 mM (XO)	n.m.	[73]
	TEA	19.9% inhibition at 1 mM (XO)	n.m.	[67]
	Quinine	17.8% inhibition at 1 mM (XO)	n.m.	[73]
	Lidocaine	13.1% inhibition at 1 mM (XO)	n.m.	[73]
	4-AP	No significant effect at 0.1–2 mM (XO)	n.m.	[67,73]
	Chloroform	44.7% inhibition at 800 μM (XO)	n.m.	[67]
	Halothane	56.4% inhibition at 800 μM (XO)	n.m.	[67]
	Isoflurane	58.4% activation at 800 μM (XO)	n.m.	[67]
	Vernakalant	Activation (XO, MC)	40 μM (MC)	[83]
	Isoflurane	Activation (XO)	162 μM (XO)	[61]
	Sevoflurane	Activation (XO)	224 μM (XO)	[61]
	Halothane	Activation (XO)	300 μM (XO)	[61]
	Desflurane	Activation (XO)	658 μM (XO)	[61]
	Dronedarone	29% activation at 100 μM (XO)	n.m.	[82]
	Loratadine	Inhibition (MC)	490 nM (MC)	[126]
	A1899 (High affinity K$_{2P}$3.1 inhibitor)	Inhibition (XO)	900 nM (XO)	[103]
	Cloxiquine	Inhibition (MC)	3.2 μM (MC)	[130]
	Zinc	Inhibition (XO)	5–10 μM for the murine but not the human ortholog	[131]
	Arachidonic acid	43% inhibition at 20 μM (MC)	6.6 μM (MC)	[73,78]
	Lamotrigine	Inhibition (MC)	47 μM (MC)	[132]
K$_{2P}$18.1 (TRESK)	Bupivacaine	~75% inhibition at 100 μM (MC)	80.4 μM (XO)	[61,133]
	Tetracaine	Inhibition (XO)	496 μM (XO)	[61]
	Ropivacaine	Inhibition (XO)	610 μM (XO)	[61]
	Chlorprocaine	Inhibition (XO)	832 μM (XO)	[61]
	Mepivacaine	Inhibition (XO)	1300 μM (XO)	[61]
	Lidocaine	~70–75% inhibition at 1 mM (MC)	3.4 mM (XO)	[61,73,78]
	Mibefradil	Inhibition at 3 μM (XO)	n.m.	[131]
	Quinidine	49% inhibition at 10 μM (MC)	n.m.	[133]
	Linoleic acid	~35% inhibition at 20 μM (MC)	n.m.	[78]
	Oleatic acid	~50% inhibition at 20 μM (MC)	n.m.	[78]
	Docosahexaenoic acid	~60% inhibition at 20 μM (MC)	n.m.	[78]
	Propafenone	95% inhibition at 50 μM (MC)	n.m.	[78]
	Glyburide	76% inhibition at 50 μM (MC)	n.m.	[78]
	Quinidine	90% inhibition at 100 μM (MC)	n.m.	[78]
	Quinine	41.9–75% inhibition at 100 μM (MC)	n.m.	[61,78]
	Etomidate	30.5% inhibition at 100 μM (XO)	n.m.	[61]
	Pentobarbital	10.4% inhibition at 100 μM (XO)	n.m.	[61]

Table 3. *Cont.*

K$_{2P}$ Channel	Drug/Compound	Effect (Organism)	EC$_{50}$ /IC$_{50}$ (Organism)	Citation
	Ketamine	14.5% inhibition at 100 μM (XO)	n.m.	[61]
	Alphaxalone	45.4% inhibition at 100 μM (XO)	n.m.	[61]
	Gabapentin	4.2% inhibition at 100 μM (XO)	n.m.	[61]
	Barium	38% inhibition at 3 mM (MC)	n.m.	[78,133]
	Ethanol	~15% inhibition at 150 mM (MC)	n.m.	[61,133]
	Apamin	No significant effect at 100 nM (XO)	n.m.	[133]
	Ruthenium red	No significant effect at 5 μM (MC)	n.m.	[133]
	Glibenclamide	No significant effect at 10 μM (MC)	n.m.	[133]
	Stearic acid	No significant effect at 20 μM (MC)	n.m.	[78]
	Digoxin	No significant effect at 100 μM (XO)	n.m.	[111]
	Digitoxin	No significant effect at 100 μM (XO)	n.m.	[111]
	Flecainide	No significant effect at 100 μM (XO)	n.m.	[84]
	Genistein	No significant effect at 100 μM (XO)	n.m.	[85]
	Tolazamide	No significant effect at 100 μM (MC)	n.m.	[78]
	Glipizide	No significant effect at 100 μM (MC)	n.m.	[78]
	Paxilline	No significant effect at 100 μM (MC)	n.m.	[78]
	Penitrem A	No significant effect at 100 μM (MC)	n.m.	[78]
	Ranolazine	No significant effect at 300 μM (XO)	n.m.	[109]
	Cesium	No significant effect at 1 mM (MC)	n.m.	[133]
	4-AP	No significant effect at 1 mM (XO)	n.m.	[73,78]
	TEA	No significant effect at 1 mM (XO) 30% inhibition at 2 mM (MC)	n.m.	[61,73,78]
	Mercury	Inhibition (XO)	n.m.	[131]
	Tetrapentyl-ammonium	Inhibition (MC)	n.m.	[130]

Potency of different drugs or compounds to activate or inhibit heterologously expressed K$_{2P}$ currents. Compounds that are used as experimental high-affinity inhibitors of individual K$_{2P}$ channels are highlighted in bold. Please note, however, that these compounds are by no means completely specific for single members of the K$_{2P}$ family. IC50, mean inhibitory concentration; MC, mammalian cells; n.m., not measured; XO, *Xenopus laevis* oocytes.

The physiological role of K$_{2P}$1.1 (TWIK-1) channel subunits has not been conclusively clarified, mostly due to lack of specific inhibitors and its very low currents in heterologous expression systems [82]. If measurable, heterologously expressed K$_{2P}$1.1 (TWIK-1) channel homodimers give rise to potassium currents that are sensitive to acidic pH as well as external K$^+$ concentration [134]. Therefore, it was speculated whether K$_{2P}$1.1 (TWIK-1) might contribute to cardiac I_{K1}, I_{KAch}, I_{KATP}, and I_{TASK} currents [11–14,80,135,136]. Altered ion conductivity under low extracellular potassium concentrations (for example Na$^+$ permeability, which shifts homodimeric K$_{2P}$1.1 (TWIK-1) channels from an inhibitory to an excitatory channel) could link K$_{2P}$1.1 (TWIK-1) channels to the pathophysiology of hypokalemia-induced rhythm disturbances [137]. Through its ability to heterodimerize with other K$_{2P}$ subunits, K$_{2P}$1.1 (TWIK-1) subunits could modulate the pharmacological and functional properties of atrial K$_{2P}$3.1 (TASK-1) channel subunits [138–140].

4. K$_{2P}$2.1 (TREK-1)

Mechanosensitivity is a unique feature of the TREK/TRAAK subfamily, as these K$_{2P}$ channels are activated by membrane stretch and osmotic swelling [141]. Temperature, lipids, extracellular or intracellular pH, anesthetics or other drugs, phosphorylation, glycosylation, G protein-coupled receptors and other protein partners represent further regulators of homodimeric K$_{2P}$2.1 (TREK-1) channels [97,124,141–144]. The versatility of this channel is further enhanced by alternative translation initiation (ATI) variants that

differ in spatiotemporal expression, single-channel conduction, ion selectivity and regarding their pharmacological profile [43,145,146]. Further, $K_{2P}2.1$ (TREK-1) channel subunits are reported to from heterodimers with $K_{2P}1.1$ (TWIK-1), $K_{2P}4.1$ (TRAAK) and $K_{2P}10.1$ (TREK-2) [147,148].

In the rat heart, *Kcnk2* mRNA and protein expression has been described in both atrial and ventricular tissue samples (Table 2) [28,29,32,33,149]. However, in the mouse heart, most studies describe ventricular-dominant $K_{2P}2.1$ (TREK-1) expression or mRNA abundance patterns [16,26,41]. Abundant $K_{2P}2.1$ (TREK-1) expression was also detected in the porcine heart, with the highest expression levels in the sinoatrial and atrioventricular nodal tissue [36,37] and in human cardiac tissue samples, where again ventricular dominant $K_{2P}2.1$ (TREK-1) expression could be observed [10,37,40,41]. Interestingly, a transmural gradient of ventricular $K_{2P}2.1$ (TREK-1) expression levels was described with endocardial expression levels 17-fold higher than that in the epicardium, [30,149]. Strikingly, this gradient seems to parallel transmural changes in stretch-activated potassium currents, as mechanical stretch has been shown to cause increased action potential shortening in subendocardial cardiomyocytes compared to the subepicardium [150]. In a similar fashion chloroform-activated $K_{2P}2.1$ (TREK-1)-like currents are significantly larger in endocardial than epicardial cells [30].

Homodimeric $K_{2P}2.1$ (TREK-1) channels are inhibited by the anticonvulsant drugs valproate, gabapentin and carbamazepine [102] by the antidepressants like fluoxetine, paroxetine, citalopram or escitalopram (Table 3) [96,102], and the antipsychotics haloperidol or clozapine [101]. While some of these interactions would only be relevant at supratherapeutic plasma levels, others already have an impact in the physiological range [141]. It has therefore been speculated whether the blockade of cardiac $K_{2P}2.1$ (TREK-1) channels could contribute to the proarrhythmic potential of these compounds [41,141]. Remarkably, $K_{2P}2.1$ (TREK-1) knockout was shown to cause a phenotype of QT interval prolongation, linking loss of cardiac $K_{2P}2.1$ (TREK-1) to QT prolongation [151]. Likewise, antiarrhythmic drugs were described to block $K_{2P}2.1$ (TREK-1) channels: Vaughan Williams class I compounds lidocaine, mexiletine and propafenone, class III antiarrhythmic drugs dronedarone and vernakalant, the beta-blocker carvedilol and late sodium current inhibitor ranolazine were identified as in vitro $K_{2P}2.1$ (TREK-1) inhibitors (Table 3) [43,82,84,104,106,109]. Since IC_{50} levels are mostly in the supratherapeutic range, it is unclear to what extent inhibition of $K_{2P}2.1$ (TREK-1) contributes to the antiarrhythmic effects of these compounds.

In isolated rat ventricular cardiomyocytes the mechano-, pH-, and arachidonic acid-sensitive potassium current I_{KAA} displays a number of further features like activation by volatile anesthetics, inhibition by cAMP analogues as well as beta-adrenergic receptor agonists, the absence of a relevant voltage dependency, a specific single-channel conductance and burst mode activity, which identify it as a $K_{2P}2.1$ (TREK-1) current (Table 4) [7,28,29,32,33,149,152]. Further, resting membrane potentials of chicken embryo-derived atrial cardiomyocytes are regulated by $K_{2P}2.1$ (TREK-1) [153]. Finally, cardiomyocyte-specific $K_{2P}2.1$ (TREK-1) knockout mice exhibit a phenotype of stress-induced sick sinus syndrome and prolongation of QT intervals that could be reproduced in a transgenic model which employed C-terminal truncation of beta IV spectrin to disrupt its interaction with $K_{2P}2.1$ (TREK-1), thereby impairing intracellular $K_{2P}2.1$ (TREK-1) protein trafficking [27,151]. In a similar fashion, knockout of $K_{2P}2.1$ (TREK-1) channel surface targeting by its protein partners POPDC1 or POPDC2 revealed a phenotype of exercise-induced and age-dependent sick sinus syndrome [154,155], while a double-knockout mouse displayed AV conduction disturbance [156]. Moreover, a familial autosomal recessive POPDC1 mutation has been associated with the phenotype of limb-girdle muscular dystrophy type X2 in combination with AV block [157] and POPDC2 mutations have been shown to cause AV block without a skeletal muscle phenotype [158].The fact that $K_{2P}2.1$ (TREK-1) channels are activated in acidosis and by mechanical stress has given rise to speculation about a role of this channel in the development of cardiac arrhythmias for more than two decades [28]. Metabolic changes associated with myocardial ischemia lead to a decrease in pH. By activating $K_{2P}2.1$ (TREK-1), this can

cause a dispersion of repolarization and consecutively the development of arrhythmias. Similarly, altered wall tension due to hypertension, valvular vitiation, in the margins of myocardial scars, or AF may activate $K_{2P}2.1$ (TREK-1) [141,158,159]. Recently, a heterozygous missense mutation (I267T) of $K_{2P}2.1$ (TREK-1) was identified in a patient with idiopathic right ventricular outflow tract tachycardia [160]. This mutation results in an amino acid exchange from isoleucine to threonine in close proximity to the selectivity filter of the channel, leading to increased stretch sensitivity and sodium permeability.

Table 4. Functional evidence for K_{2P} channel expression in the cardiovascular system.

K_{2P} Channel Subunit	Species	Population/Model/Methodology	Observation	Citation
$K_{2P}1.1$ (TWIK-1)	Zebrafish	Morpholino knockdown mRNA (RT-PCR, ISH)	Knockdown of *kcnk1a* or *kcnk1b* in zebrafish embryos resulted in a phenotype atrial dilatation and bradycardia	[11]
	Mouse	CREM-transgenic murine AF model mRNA (RT-qPCR, TaqMan)	Moderate cardiac mRNA expression, V > A Ventricular mRNA downregulated in murine AF model	[16]
	Rat	Goto-Kakizaki type 2 diabetic ratsmRNA (RT-qPCR, TaqMan)	Downregulation of sinoatrial mRNA levels in Goto-Kakizaki type 2 diabetic rats	[19]
	Human	Patient-derived tissue samples mRNA (RT-PCR)	Identical mRNA levels in failing and healthy hearts	[21]
	Human	Patient-derived tissue samples	Upregulation of atrial mRNA levels in patients with atrial dilatation	[11]
	Human	Patient-derived tissue samples	Upregulation of atrial mRNA levels in patients with Brugada syndrome	[80]
	Human	Patient-derived tissue samples	Downregulation of atrial mRNA levels in AF	[12]
	Human	AF patients	Identification of three non-synonymous *KCNK1* gene variants (p.R171H, p.I98M, and p.G236S) in a cohort of 373 atrial fibrillation (AF) patients	[11]
	Human	mRNA (RT-qPCR, TaqMan)	No regulation of atrial mRNA levels in AF	[10]
$K_{2P}2.1$ (TREK-2)	Mouse	CREM-transgenic murine AF model Murine TAC model mRNA (RT-qPCR, TaqMan)	Upregulated of atrial and ventricular mRNA in a murine AF model Downregulation of atrial and ventricular mRNA in a murine TAC model	[16]
	Rat	Rat model of isoproterenol-induced left ventricular hypertrophy	Increased protein levels upon isoproterenol stimulation	[149]

K$_{2P}$ Channel Subunit	Species	Population/Model/Methodology	Observation	Citation
	Mouse	Protein (IF)	Global K$_{2P}$2.1 (TREK-1) knockout mice showed an exaggerated form of pressure overload-induced concentric ventricular hypertrophy, which could be prohibited only by fibroblast-specific deletion of K$_{2P}$2.1, (TREK-1) whereas the cardiomyocyte-specific knockout of K$_{2P}$2.1 (TREK-1) resulted in cardiac dysfunction under pressure-overload conditions	[161]
	Human	Patient-derives tissue samples mRNA (RT-qPCR, TaqMan)	Downregulation of atrial mRNA in AF	[37]
	Pig	Large animal model of burst pacing-induced AF and heart failure	Downregulation of atrial mRNA and protein Attenuation of the AF phenotype by KCNK2 gene therapy	[36,37]
	Rat	Goto-Kakizaki type 2 diabetic ratsmRNA (RT-qPCR, TaqMan)	Upregulation of sinuatrial mRNA levels in Goto-Kakizaki type 2 diabetic rats	[19]
	Human	Index patient	A heterozygous missense mutation (I267T) of K$_{2P}$2.1 (TREK-1) was identified in a patient with idiopathic right ventricular outflow tract tachycardia	[160]
	Chicken	Isolated atrial cardiomyocytes	Resting membrane potentials of chicken embryo-derived atrial cardiomyocytes are regulated by K$_{2P}$2.1	[153]
	Rat	Isolated rat ventricular cardiomyocytes	In isolated rat ventricular cardiomyocytes the mechano-, pH-, and arachidonic acid-sensitive potassium current I_{KAA} displays a number of characteristics which identify it as a K$_{2P}$2.1 (TREK-1) current	[7,28,29,32,33, 149,152]
	Mouse	*Kcnk2* knockout mouse	Phenotype of QT interval prolongation and sick sinus syndrome	[35]
K$_{2P}$3.1 (TASK-1)	Rat	Isolated rat ventricular cardiomyocytes	K$_{2P}$3.1 (TASK-1) currents were isolated from rat ventricular cardiomyocytes by lowering pH, activation of cardiac α1-adrenergic receptors and by administration of the inhibitor A293	[15,162,163]
	Mouse	Isolated cardiomyocytes	Patch-clamp measurements of K$_{2P}$3.1 (TASK-1) currents (controlled by knockout mice)	[45]
	Pig	Isolated atrial cardiomyocytes	Patch-clamp measurements of K$_{2P}$3.1 (TASK-1) currents using A293: APD prolongation via K$_{2P}$3.1 (TASK-1) inhibition	[52–54,164]

Table 4. *Cont.*

K$_{2P}$ Channel Subunit	Species	Population/Model/Methodology	Observation	Citation
	Human	Isolated atrial cardiomyocytes	Patch-clamp measurements of K$_{2P}$3.1 (TASK-1) currents using A293: APD prolongation via K$_{2P}$3.1 (TASK-1) inhibition I_{TASK-1} was identified to carry up to 28% of the background potassium current in isolated human atrial cardiomyocytes	[10,39,40,53, 56].
	Human	iPSC	Prolongation of APD values by transfection of K$_{2P}$3.1 (TASK-1) siRNA	[22]
	Zebrafish	Morpholino knockdown	Decreased heart rate was observed after K$_{2P}$3.1 (TASK-1) knockdown	[165].
	Mouse	CREM-transgenic murine AF model Murine TAC model mRNA (RT-qPCR, TaqMan) and protein (WB)	Downregulation of atrial mRNA and protein level in murine AF model Downregulation of atrial mRNA and protein level in murine TAC model	[16]
	Guinea pig	Excised guinea pig hearts	Prolongation of atrial effective refractory periods upon TASK-1 inhibition at pH 7.8	[49]
	Mouse	*Kcnk3* knockout mouse	Phenotype of QTc prolongation (around 30%), prolongation of single cell APDs or monophasic action potentials and a broad QRS complex	[47]
	Rat	*Kcnk3* knockout rat	Phenotype of cardiomyocyte APD prolongation as well as resting membrane depolarization	[15]
	Dog	Dog model of postoperative AF	Downregulation of atrial TASK-1 expression in postoperative AF	[50]
	Pig	Large animal model of burst pacing-induced AF	Upregulation of atrial TASK-1 expression and currents Acute cardioversion upon TASK-1 inhibition Rhythm control of AF upon TASK-1 gene therapy of pharmacological TASK-1 inhibition	[52,141,164]
	Human	mRNA (RT-qPCR, TaqMan), protein (WB)	Upregulation of atrial TASK-1 expression and currents in cAF	[10,41,55,57]
	Human	AF patient cohort	Three genetic *KCNK3* variants which reduce the expression or channel function were found in patients with familial AF	[49]
	Mouse	*Kcnk3* knockout mouse	Compared to wild-type littermates, *Kcnk3* knockout mice showed a preservation of systolic as well as diastolic function and a relative abrogation in concentric left ventricular hypertrophy upon TAC-induced pressure overload	[46]

Table 4. *Cont.*

K₂ₚ Channel Subunit	Species	Population/Model/Methodology	Observation	Citation
	Human	Patient cohorts	*KCNK3* loss-of-function mutations were found to cause idiopathic pulmonary arterial hypertension	[166]
	Human	Patient-derived tissue samples mRNA (RT-qPCR, TaqMan) and protein (WB)	Upregulation of atrial mRNA and protein in AF Downregulation of atrial mRNA in heart failure	[40]
K₂ₚ4.1 (TRAAK)	Mouse	*Kcnk4* knockout mice	No obvious cardiac phenotype reported	[167,168]
	Human	Patient-derived tissue samples mRNA (RT-qPCR)	Downregulation of ventricular mRNA levels in non-ischemic heart failure	[22]
	Human	Patient-derived tissue samples mRNA (RT-qPCR, TaqMan)	No regulation of atrial mRNA levels in AF patients	[10]
K₂ₚ5.1 (TASK-2)	Mouse	*Kcnk5* knockout mice	Observation of subviable phenotype and sudden unexplained dead but association with arrhythmia or cardiomyopathy remains speculative as no detailed cardiac characterization was reported	[169]
	Mouse	CREM-transgenic murine AF model mRNA (RT-qPCR, TaqMan)	No regulation of atrial mRNA in murine AF model	[16]
	Rat	Goto-Kakizaki type 2 diabetic rats mRNA (RT-qPCR, TaqMan)	Downregulation of sinoatrial mRNA levels in Goto-Kakizaki type 2 diabetic rats	[19]
	Human	mRNA (RT-qPCR, TaqMan)	Trend towards downregulation of atrial mRNA levels in AF	[10]
K₂ₚ6.1 (TWIK-2)			*Physiological role under debate because of low currents upon recombinant expression*	
	Mouse	CREM-transgenic murine AF model Murine TAC model mRNA (RT-qPCR, TaqMan)	No regulation in murine AF model Upregulation of atrial mRNA in murine TAC model	[16]
	Rat	Goto-Kakizaki type 2 diabetic rats mRNA (RT-qPCR, TaqMan)	Downregulation of sinoatrial mRNA levels in Goto-Kakizaki type 2 diabetic rats	[19]
	Mouse	*Kcnk6* knockout mouse	*Kcnk6* knockout mice are hypertensive and display elevated RV pressure level as well as enhanced vascular contractility	[170–172]
	Human	Patient-derived tissue samples mRNA (RT-qPCR, TaqMan)	No regulation of atrial mRNA in AF patients	[10]
K₂ₚ7.1 (TWIK-3)	Human, Mouse	mRNA (RT-qPCR, TaqMan)	*Most studies show very low cardiac mRNA levels. Functionality of the channel still under debate.*	[16] al. 2015) Wang et al. 2018)
	Human	Patient-derived tissue samples mRNA (RT-qPCR)	Upregulation of atrial mRNA levels in AF	[63]

Table 4. *Cont.*

K$_{2P}$ Channel Subunit	Species	Population/Model/Methodology	Observation	Citation
	Human	Patient-derived tissue samples mRNA (RT-qPCR, TaqMan)	No mRNA regulation in AF	[10]
K$_{2P}$9.1 (TASK-3)	Mouse	*Kcnk7* knockout mouse	No cardiac phenotype of the *Kcnk7* knockout mouse has been described	[173]
	Human	Genetic disease	*KCNK9* imprinting syndrome linked to obstructive sleep apnea	
	Human	Patient-derived tissue samples mRNA (RT-qPCR)	Downregulation of ventricular mRNA levels in heart failure	[22]
	Human	Patient-derived tissue samples mRNA (RT-qPCR, TaqMan)	Trend towards upregulation in AF	[10]
	Mouse	*Kcnk9* knockout mouse	Phenotype of concentric left ventricular hypertrophy with preserved ejection fraction	[46]
	Human	Single channel patch-clamp measurements on isolated human atrial cardiomyocytes	Evidence for heteromeric K$_{2P}$9.1/ K$_{2P}$3.1 but not for K$_{2P}$9.1 homodimers	[56]
K$_{2P}$10.1 (TREK-2)	Human, mouse	Patient-derived tissue samples, CREM-transgenic murine AF model, Murine TAC model, mRNA (RT-qPCR, TaqMan)	No regulation of atrial mRNA levels in AF patientsNo regulation of atrial or ventricular mRNA levels in a murine AF modelNo changes in ventricular mRNA levels in a murine TAC modelUpregulation of left and right atrial mRNA in heart failure patients	[41]
	Mouse	*Kcnk10* knockout mouse	No cardiac phenotype of the *Kcnk10* knockout mouse has been described	[174]
	Human	Patient-derived tissue samples mRNA (RT-qPCR, TaqMan)	No regulation of atrial mRNA levels in AF patients	[10]
K$_{2P}$12.1 (THIK-2)	Human, Rat, Mouse	mRNA (NB, RT-PCR, RT-qPCR, TaqMan)	*Most studies showvery low cardiac mRNA levels. Functionality of the channel still under debate.*	[10,15,16,66, 67]
K$_{2P}$13.1 (THIK-1)	Human	Patient-derived tissue samples mRNA (RT-qPCR, TaqMan)	Downregulation of atrial mRNA level in cAF patients	[10]
	Human	Patient-derived tissue samples mRNA (RT-qPCR, TaqMan)	Trend towards downregulation of atrial mRNA level in heart failure patients	[40]
K$_{2P}$15.1 (TASK-5)	Pig	Large animal model of burst-pacing induced AF and heart failure	Downregulation of atrial protein expression in combined AF and heart failure	[129]
	Human, Rat, Mouse	mRNA (RT-PCR, RT-qPCR)	*Most studies showrather low cardiac mRNA levels. Functionality of the channel still under debate.*	[10,15,69,70] Wiedmann et al. 2018)
	Human	Patient-derived tissue samples mRNA (RT-qPCR, TaqMan)	No regulation of atrial mRNA levels in cAF patients	[10]
K$_{2P}$16.1 (TALK-1)	Mouse	CREM-transgenic murine AF model mRNA (RT-qPCR, TaqMan)	Downregulation of atrial mRNA levels in murine AF model	[16]
	Human, Rat	mRNA (NB, RT-PCR, RT-qPCR, TaqMan)	*Most studies shownegligible or low cardiac mRNA levels*	[10,15,60,67, 71]

Table 4. *Cont.*

K$_{2P}$ Channel Subunit	Species	Population/Model/Methodology	Observation	Citation
K$_{2P}$17.1 (TALK-2)	Human	Patient-derived tissue samples, iPSC mRNA (RT-qPCR)	Downregulation of ventricular mRNA levels in non-ischemic heart failure iPSC: *KCNK17* knockdown led to APD prolongation	[22]
	Human, Mouse	Index patient HL-1 cells (cultured cardiomyocyte cell line), mRNA (RT-qPCR)	A patient suffering from progressive and severe cardiac conduction disorder in combination with idiopathic ventricular fibrillation was identified to carry both, a splice site mutation in the sodium channel gene *SCN5A* as well as a gain-of-function mutation in the *KCNK17* gene HL-1 cells: KCNK17 *knockdown* overexpression led to APD shortening	[5]
	Human	Index family Patient derived iPSC	A common *KCNK17* gain-of-function variant might be protective for LQTS by promoting APD shortening	[74]
	Human	Patient-derived tissue samples, mRNA (RT-qPCR, TaqMan)	Downregulation of right atrial mRNA levels in cAF	[10]
	Human	Patient-derived tissue samples, mRNA (RT-qPCR, TaqMan) and protein (WB)	Downregulation of left and right atrial protein and mRNA level in HF	[40]
K$_{2P}$18.1 (TRESK)	Zebrafish, Mouse, Human	mRNA (ISH, RT-PCR, RT-qPCR, TaqMan)	*Most studies shownegligible cardiac mRNA levels*	[10,16,61,76–78]

Evidence in literature for cardiac relevance of K$_{2P}$ channel subunits. A, expression in atrial tissue; AF, atrial fibrillation; HF, heart failure; IF, immunofluorescence; iPS, induced pluripotent stem cell; ISH, in situ hybridization; LA, left atrium; NB, Northern blot; RT-PCR, reverse transcriptase PCR; RT-qPCR, reverse transcriptase quantitative PCR; RA, right atrium; TAC, transverse aortic constriction; TaqMan, reverse transcriptase quantitative PCR employing TaqMan® hydrolyse probes to increase specificity; V, expression in ventricular tissue; WB, Western blot.

In a murine model of transverse aortic constriction (TAC)-induced pressure overload upregulation of ventricular *Kcnk2* mRNA expression was described [16]. In a similar fashion, K$_{2P}$2.1 (TREK-1) protein levels were increased in a rat model of isoproterenol-induced left ventricular hypertrophy [149]. Global K$_{2P}$2.1 (TREK-1) knockout mice showed an exaggerated form of pressure overload-induced concentric ventricular hypertrophy, which could be prohibited only by fibroblast-specific deletion of K$_{2P}$2.1, (TREK-1) whereas the cardiomyocyte-specific knockout of K$_{2P}$2.1 (TREK-1) resulted in cardiac dysfunction under pressure-overload conditions [161]. In a murine atrial fibrillation (AF) model of CREM-IbΔC-X transgenic mice, downregulation of atrial K$_{2P}$2.1 (TREK-1) mRNA and protein levels were observed [16,41]. It, however, remains uncertain whether this is also the case for AF patients: while one study described AF-associated downregulation of atrial K$_{2P}$2.1 (TREK-1) [37] others merely describe a trend that does not reach statistical significance [10,40,41]. One possible explanation is the remote regulation of atrial K$_{2P}$2.1 (TREK-1) expression by ventricular heart failure, a mechanism recently described for K$_{2P}$3.1 (TASK-1) [40] and also observed for K$_{2P}$2.1 (TREK-1) in another study [41]. Indeed, in contrast to the other study, the cohort of patients characterized in the former study was performed in patients who all suffered from severe heart failure. In a similar fashion, a strong trend towards downregulation of atrial *Kcnk2* mRNA could be observed in a murine

model of TAC-induced pressure overload [16]. Furthermore, downregulation of atrial $K_{2P}2.1$ (TREK-1) protein expression was described in a porcine model of combined AF and heart failure [36] and gene therapeutic restoraton of $K_{2P}2.1$ (TREK-1) expression was able to attenuate the AF phenotype [37].

For a more detailed description of the cardiac role of $K_{2P}2.1$ (TREK-1), we would like to refer to the following literature [41,141,158].

5. $K_{2P}3.1$ (TASK-1)

Among the entire K_{2P} family, $K_{2P}3.1$ (TASK-1) is the channel with the best characterized cardiac significance. $K_{2P}3.1$ (TASK-1) channels are expressed in neuronal tissue, cardiomyocytes, vascular smooth muscle cells, the carotid body glomus, the adrenal gland, brown adipose tissue and immunocytes, where they control important physiological processes [2,115]. $K_{2P}3.1$ (TASK-1) channels are regulated by a number of different stimuli, such as pH level, hypoxia, PKA, PKC, or PLC activity, and several drugs like volatile anesthetics [2].

In the murine and the rat heart, *KCNK3* mRNA was detected, both in atrial as well as in ventricular tissue samples (Northern blot, RT-PCR, Taq-Man qPCR; Table 2) [15,16,18,25,26,34,44,45,47]. Humans, however, show an almost atrial-specific $K_{2P}3.1$ (TASK-1) expression within the heart with 14- to 16-fold lower expression levels in ventricular tissue (RT-PCR, Taq-Man qPCR, microarray, bulk RNAseq, Western blot) [10,12,14,39,40,49,54,56,57]. In guinea pigs and domestic swine, atrial-specific $K_{2P}3.1$ (TASK-1) expression was also described [49,51–54].

Several clinically relevant antiarrhythmic drugs have been identified to inhibit homodimeric $K_{2P}3.1$ (TASK-1) channels at either physiological or subtherapeutic concentrations (Table 3). Among them are the class I antiarrhythmic drugs propafenone, mexiletine, lidocaine, and quinidine [104,122,123], the betablockers propranolol and carvedilol [42], class III antiarrhythmics amiodarone and dronedarone [82,110] as well as cardiac glycosides [111] and ranolazine [109]. The respiratory stimulant doxapram was further identified as a potent blocker of both $K_{2P}3.1$ (TASK-1) and $K_{2P}9.1$ (TASK-3) channels through which it presumably exerts the main part of its respiratory drive-increasing effect [119,175]. Furthermore, preclinical experimental antiarrhythmic drugs developed as specific inhibitors of the $K_V1.5$ channel (A239 [AVE1231], A1899 [S20591], AVE0118, S9947, MSD-D, and ICAGEN-4) are potent $K_{2P}3.1$ (TASK-1) inhibitors [117]. Although no direct structural similarities of the pore regions of both channels could be detected, these compounds were shown to be 1.4- to 70-fold more potent $K_{2P}3.1$ (TASK-1) inhibitors as compared to $K_V1.5$ [117]. In addition, bisamides represent a new class of high-affinity $K_{2P}3.1$ (TASK-1) inhibitors with IC_{50} values in the single-digit nanomolar range, as in the case of compound ML365 (Table 3) [116].

Availability of high-affinity inhibitors enables functional detection of $K_{2P}3.1$ (TASK-1) currents in isolated cardiomyocytes. $K_{2P}3.1$ (TASK-1) currents were isolated from rat ventricular cardiomyocytes by lowering pH, activation of cardiac α1-adrenergic receptors and by administration of the inhibitor A293 (Table 4) [15,162,163]. Patch-clamp measurements of murine $K_{2P}3.1$ (TASK-1) current could be confirmed by the use of *Kcnk3* knockout mice [25] and likewise, functional detection of $K_{2P}3.1$ (TASK-1) currents was achieved by patch-clamp technique in isolated porcine [52–54,164] and human atrial cardiomyocytes, where a significant APD prolongation could be demonstrated [10,39,40,53,56]. Under physiological conditions, I_{TASK-1} was identified to carry up to 28% of the background potassium current in isolated human atrial cardiomyocytes [39].

In induced pluripotent stem cell- (iPS-) derived cardiomyocytes (iPSC), APD values could be prolonged by transfection of $K_{2P}3.1$ (TASK-1) siRNA [22]. In a zebrafish model, a decreased heart rate was observed after $K_{2P}3.1$ (TASK-1) knockdown, which was accompanied by an increased atrial diameter [165]. In excised guinea pig hearts, APD remained unchanged upon $K_{2P}3.1$ (TASK-1) inhibition with A293 or ML365. Switching the pH level from pH 7.4 to 7.8, however, resulted in significant prolongation of atrial effective refractory periods [49]. Global *Kcnk3* knockout mice exhibited a phenotype of QTc prolongation

(around 30%), prolongation of single cell APDs or monophasic action potentials and a broad QRS complex [25,26]. In transgenic *Kcnk3* knockout rats, APD prolongation as well as resting membrane depolarization was described [163].

In a porcine large animal model of AF, atrial $K_{2P}3.1$ (TASK-1) expression was found to be significantly upregulated (TaqMan qPCR, western blot, patch-clamp electrophysiology) [52,141,164]. These results could also be reproduced on atrial tissue samples from atrial fibrillation patients (TaqMan qPCR, microarray, bulk RNAseq, western blot, patch-clamp electrophysiology) [10,41,55,57]. Considering its atrial-specific expression, its effect on atrial APD, and its upregulation in patients with AF, $K_{2P}3.1$ (TASK-1) channels combine several properties that make it an ideal molecular target for the treatment of AF.

Inhibition of $K_{2P}3.1$ (TASK-1) in cardiomyocytes from AF patients has been shown to counteract AF-induced APD shortening [104,154]. After administration of A293 (200 nM), APDs of atrial cardiomyocytes isolated from AF patients could be prolonged around 30% to values observed in sinus rhythm controls [104,154]. After intravenous application of $K_{2P}3.1$ (TASK-1) inhibitors in healthy control pigs, significant prolongation of both, atrial effective refractory periods and ADP values pointed towards class III antiarrhythmic effects of $K_{2P}3.1$ (TASK-1) inhibition [53,54]. Furthermore, the inducibility of atrial arrhythmias was significantly reduced by $K_{2P}3.1$ (TASK-1) inhibitors in different studies [176–178]. In a similar fashion, intravenous administration of $K_{2P}3.1$ (TASK-1) inhibitors A293 and doxapram led to rapid, safe and successful cardioversion of artificially induced AF episodes in a porcine large animal model [53,54]. These antiarrhythmic effects could further be employed for rhythm control in a porcine model of burst pacing induced "persistent" AF, induced via implanted pacemakers using a biofeedback algorithm [53,164] and reproduced with an AAV-mediated anti-$K_{2P}3.1$ (TASK-1) gene therapy approach [52]. Based on these encouraging results, the currently ongoing DOCTOS trial (doxapram conversion to sinus rhythm; EudraCT No: 2018-002979-17) was started, which investigates whether the FDA and EMA approved $K_{2P}3.1$ (TASK-1) inhibitor doxapram can cardiovert AF in patients [2,179].

Interestingly, also reduction of atrial $K_{2P}3.1$ (TASK-1) expression was linked to AF as in a dog model of postoperative AF, a phosphorylation dependent downregulation of $K_{2P}3.1$ (TASK-1) was reported [50] and CREM-TG AF mice display atrial downregulation of $K_{2P}3.1$ (TASK-1) in conjunction with massive atrial dilatation and scarring [16]. Patients who suffer from reduced left ventricular ejection fraction display reduced atrial $K_{2P}3.1$ (TASK-1) expression, independently from their rhythm state [40]. Finally, three genetic variants (two kozak variants and missense variant $K_{2P}3.1$ (TASK-1) V123L mutation all of which reduce the expression or channel function) were found in patients with familial AF [49].

In addition to its role in the control of heart rhythm, $K_{2P}3.1$ (TASK-1) is also discussed as a regulator of cardiac energetics and metabolic function, as *Kcnk3* knockout mice were protected from pressure overload-induced cardiomyopathy. Compared to wild-type littermates, *Kcnk3* knockout mice showed a preservation of systolic as well as diastolic function and a relative abrogation in concentric left ventricular hypertrophy upon TAC-induced pressure overload [46].

Moreover, $K_{2P}3.1$ (TASK-1) channels were described to be expressed in in human pulmonary artery smooth muscle cells, where they serve as regulators of the basal membrane potential and consecutively regulate pulmonary vascular tone [180]. Furthermore, *KCNK3* loss-of-function mutations were found to cause idiopathic pulmonary arterial hypertension [166] and acute pharmacological $K_{2P}3.1$ (TASK-1) inhibition in pigs led to a mild but significant increase in invasively measured pulmonary arterial pressure [164]. In the context of adrenal *KCNK3* expression, a role of the $K_{2P}3.1$ (TASK-1) channel in aldosterone secretion and blood pressure control is further discussed. Global *Kcnk3* knockout mice display a phenotype of mild hyperaldosteronism [181] and single nucleotide polymorphisms in the *KCNK3* gene were associated with plasma aldosterone levels [182]. Accordingly, elevated systolic blood pressure values were described in the *Kcnk3* knockout mouse [25]. Finally, $K_{2P}3.1$ (TASK-1) channels are also discussed to be involved in regulating function

of immune cells and in thermogenesis in brown adipose tissue [183]. Thus, there is a need for further studies that exclude systemic side effects in the use of TASK-1 inhibitors for treatment of AF.

6. K_{2P}4.1 (TRAAK)

Although it was suspected about 20 years ago, that the K_{2P}4.1 (TRAAK) channel, based on northern blot analysis, might be mainly expressed in the human heart there is little evidence to date for a cardiac role of this K_{2P} channel. Several studies reported cardiac *KCNK4* mRNA expression, mostly with atrial predominant expression patterns (TaqMan qPCR; Table 2) in human as well as in murine heart tissue samples [10,22,26,41]. Compared with other cardiac ion channels, however, expression levels were relatively low [10,16,41]. A mild inhibitory effect of vernakalant and the late sodium channel blocker ranolazine has also been described for hK_{2P}4.1 (TRAAK) homodimeric channels (Table 3) [83,109].

Kcnk4 knockout mice were reported to display smaller ischemic areas upon cerebral infarction. No obvious phenotype of heart rhythm disorder or heart failure was described, and the mice were reported as viably and healthy [167,168]. We are, however, not aware of any studies that explicitly study the cardiac phenotype of these transgenic mice (Table 4).

7. K_{2P}5.1 (TASK-2)

Shortly after the first description of the *KCNK5* gene, RT-PCR experiments had already indicated robust cardiac abundance of *KCNK5* mRNA [184], while other studies (RT-PCR) considered the cardiac mRNA levels to be rather low (Table 2) [22,23,26,38]. Our own studies indicated atrial predominant *KCNK5* mRNA abundance within the human and murine heart [10,16]. Further, a trend towards downregulation of atrial *KCNK5* mRNA in patients, suffering from chronic AF was noted that did not reach statistical significance [10]. K_{2P}5.1 (TASK-2) homodimers are a molecular target on volatile and amide type local anesthetics (Table 3) [185,186] and inhibited by supratherapeutic concentrations of ranolazine [109]. siRNA transfection experiments pointed towards a functional role of K_{2P}5.1 (TASK-2) in setting the membrane potential of pulmonary artery myocytes [187]. In the diabetic rat model with sinus bradycardia, mentioned above, downregulation of cardiac *Kcnk5* mRNA expression was reported (Table 4) [19]. Finally, genome-wide association studies could identify a risk locus, associated with the development of coronary artery disease and migraine within the *KCNK5* gene [188].

Breeding of global *Kcnk5* knockout mice resulted in a small number of female homozygous offspring, pointing towards a phenotype which might cause antenatal mortality [169]. Further, Gerstin et al. reported that one homozygote female animal was found dead in the cage at 12 days of age [169]. However, whether this was associated with cardiomyopathy or arrhythmia remains speculative.

8. K_{2P}6.1 (TWIK-2)

Robust cardiac expressions patterns of *KCNK6* mRNA, derived from RT-PCR were described [10,18,22], while others report mild to moderate cardiac expression of this channel (RT-PCR, WB; Table 2) [15,23,26]. Interestingly, mRNA levels were reported to be significantly higher in the adult as compared to the neonatal rat heart [18]. Furthermore, abundant *Kcnk6* mRNA levels were found in rat saphenous arteries [189]. Upon TAC-induced pressure overload, an upregulation of murine ventricular *Kcnk6* mRNA could be observed (Table 4) [16]. *Kcnk6* deficient mice are hypertensive and display elevated RV pressure level as well as enhanced vascular contractility which was linked to enhanced rho kinase activity [170–172]. The physiological relevance of K_{2P}6.1 (TWIK-2) is under debate because these channels conduct only low currents in the heterologous expression system [82]. It further was recently reported that K_{2P}6.1 (TWIK-2) channel subunits give rise to functional K_{2P} currents in endolysosomes, where they affect the size and number of lysosomes [190] so it remains unclear whether the cell membrane is indeed the actual site of action of these channels.

9. K$_{2P}$7.1 (TWIK-3)

The mainly neuronally detected K$_{2P}$7.1 (TWIK-3) channel is a silent K$_{2P}$ channel without proven potassium conductance in heterologous expression systems [191]. Only very low cardiac expression levels have been described for *KCNK7* (RT-PCR, TaqMan qPCR; Table 2) [10,23]. It was, however speculated whether its mRNA expression might be up-regulated in atrial tissue samples, derived from AF patients [63]. Although not explicitly cardiac characterized, a global *Kcnk7* knockout mouse showed no obvious cardiac phenotype. Homozygous transgenic mice and wild-type littermates did not differ significantly in general appearance, gross anatomy, locomotion, or overt behavior (Table 4) [173].

10. K$_{2P}$9.1 (TASK-3)

The cardiac relevance of K$_{2P}$9.1 (TASK-3) channel subunits which are primarily known for their role in apoptosis, aldosterone secretion and tumor genesis remains controversial. Whereas most studies detected only relatively low mRNA levels in the human heart (qPCR, TaqMan qPCR; Table 2) [10,22,26,49], others showed high atrial expression, almost comparable to K$_{2P}$3.1 (TASK-1) (RT qPCR, IF) [56]. In the rodent heart, low *Kcnk9* (TASK-3) mRNA abundance been described [15,16,18,25,26,48].

Echocardiographic characterization of *Kcnk9* knockout mice revealed a phenotype of concentric left ventricular hypertrophy with preserved ejection fraction (Table 4) [46]. In contrast to *Kcnk3* knockout mice, however, these animals are not TAC resistant, and heart failure symptoms are more likely to occur at a later time point [46]. Downregulation of ventricular *KCNK9* mRNA expression (TaqMan qPCR) in heart failure patients might point towards a pathophysiological role of this channel [22].

Single channel patch-clamp measurements, performed in isolated human atrial cardiomyocytes were able to detect a channel with characteristics corresponding to a heteromer of K$_{2P}$3.1 (TASK-1) and K$_{2P}$9.1 (TASK-3) [56]. However, besides this heteromeric and homodimeric K$_{2P}$3.1 (TASK-1) channels, no current corresponding to a homodimeric K$_{2P}$9.1 (TASK-3) channels could be detected. Functional studies in motoneurons or in rat carotid body glomus cells indicate that the K$_{2P}$3.1 (TASK-1)/ K$_{2P}$9.1 (TASK-3) heterodimer portion was about 52–75% and thus only a minority of K$_{2P}$3.1 (TASK-1) channels are expressed as monomer at the cell surface [192,193]. Since the pharmacological properties of homodimeric and heterodimeric channels differ, heterodimerization has to be taken into account when targeting the K$_{2P}$3.1 (TASK-1) channel in the treatment of cardiac arrhythmias.

A rare genetic disease, *KCNK9* imprinting syndrome, also known as Birk-Barel Syndrome is inherited in an autosomal dominant, maternally imprinted manner and associated with congenital central hypotonia, severe feeding difficulties, delayed development, and dysmorphic manifestations [194]. While no direct cardiac manifestation has been described to date, affected individuals may develop obstructive sleep apnea syndrome, which is particularly interesting because it again links the K$_{2P}$ channels of the TASK subfamily to this disease entity.

Together with K$_{2P}$3.1 (TASK-1), K$_{2P}$9.1 (TASK-3) contributes to peripheral and central respiratory regulation [195]. Therefore, these K$_{2P}$-channels are likely to constitute a molecular target of the respiratory stimulant doxapram [53]. K$_{2P}$9.1 (TASK-3) homodimers are further inhibited by the class III antiarrhythmic drug dronedarone [82] and the antianginal drug ranolazine [109].

Hopefully, the recently available high-affinity K$_{2P}$9.1 (TASK-3) inhibitors and activators will help to answer the question of the functional relevance of K$_{2P}$9.1 (TASK-3) channels in cardiomyocytes.

11. K$_{2P}$10.1 (TREK-2)

The role of K$_{2P}$10.1 (TREK-2) channel subunits has so far been characterized mainly in the central nervous system (CNS), where this channel shows ubiquitous expression. However, a *KCNK10* knockout mouse showed remarkably few neurobehavioral phenotypes besides discrete abnormalities in anxiety-related behavior [174]. A cardiac phenotype

of this mouse has not been described yet. Pharmacological in vitro measurements revealed vernakalant and carvedilol as inhibitors of $K_{2P}10.1$ (TREK-2) homodimer channels (Table 3) [43,83]. Low cardiac mRNA abundance was described by our group and others (RT-PCR, TaqMan qPCR; Table 2) [10,15,22,40]. However, the expression patterns appeared atrial-predominant both in murine and patient-derived samples [10,41]. No relevant changes of $K_{2P}10.1$ (TREK-2) expression could be detected in murine disease models of TAC-induced pressure overload or CREM-TG AF (Table 4) [16]. However, in right and left atrial patient-derived tissue samples, significant mRNA upregulation was demonstrated upon systolic heart failure [41].

12. $K_{2P}12.1$ (THIK-2)

$K_{2P}12.1$ (THIK-2) is referred to as a silent K_{2P}-channel. This is likely due to both, a N-terminal retention signal and a low endogenous open probability [196]. While cardiac $K_{2P}12.1$ (THIK-2) mRNA levels (RT-PCR, TaqMan qPCR) were described to be rather low (Table 2) [10,15,16,67], $K_{2P}12.1$ (THIK-2) expression was detected in rat saphenous arteries [189] and might therefore be of relevance in control of vascular tone.

13. $K_{2P}13.1$ (THIK-1)

$K_{2P}13.1$ (THIK-1) mRNA was described in the CNS, arterial smooth muscle cells, the kidney and myocardial tissue samples via RT-PCR [15,22,26,66,68]. In patient-derived myocardial tissue samples, *KCNK13* mRNA abundance (TaqMan qPCR) could be demonstrated with atrial predominance (Table 2) [10]. Heterologously expressed $K_{2P}13.1$ (THIK-1) channel homodimers were inhibited by the antiarrhythmic drugs lidocaine, mexiletine, propafenone and propranolol, while administration of quinidine, amiodarone, dronedarone or ranolazine resulted in a mild channel activation (Table 3) [82,109,129].

The observation of reduced *KCNK13* mRNA levels in patients with chronic AF or heart failure, which could also be recapitulated in a porcine large animal model of combined AF and heart failure might point towards a physiological role of $K_{2P}13.1$ (THIK-1) currents in regulating atrial electrophysiology [10,40,129]. Finally, ventricular expression levels of *KCNK13* mRNA, were described as unchanged in heart failure patients (Table 4) [22].

14. $K_{2P}15.1$ (TALK-5)

Data on cardiac expression of $K_{2P}15$ (TASK-5) remain sparse. While some work has shown evidence of *KCNK15* mRNA abundance in rodent hearts (RT-PCR), very low levels of mRNA at best have been detected in human (northern blot, RT-PCR, TaqMan qPCR; Table 2) [10,26,48,69,70] or rodent (RT-PCR, TaqMan-qPCR) [15,16,26] heart samples by other groups. Downregulation of atrial *KCNK15* mRNA was reported in a murine CREM-TG model of AF (Table 4) [16]. Finally, functionality of $K_{2P}15$ (TASK-5) channel subunits is still controversial, as recombinantly expressed $K_{2P}15$ (TASK-5) homodimers do not give rise to potassium currents [8].

15. $K_{2P}16.1$ (TALK-1)

$K_{2P}16.1$ (TALK-1) is primarily expressed in pancreatic beta cells, where it is supposed to regulate insulin secretion. Recently, a gain of function mutation in *KCNK16* was identified to cause maturity-onset diabetes of the young [197]. Five studies showed low to negligible abundance of *KCNK16* mRNA in human or rat cardiac tissue samples (Table 2) [10,15,60,67,71]. Upon heterologous expression in *Xenopus laevis* oocytes, homodimeric $K_{2P}16.1$ (TALK-1) channels are inhibited by ranolazine (Table 3) [109].

16. $K_{2P}17.1$ (TALK-2)

$K_{2P}17.1$ (TALK-2) channel subunits are expressed in the human heart (northern blot, RT-PCR, Taq-Man qPCR, western blot) [5,10,22,40,67,73,75] and in patient-derived iPSC (RT-PCR, qPCR, IF) [22,74]. Cardiac mRNA levels of *KCNK17* were described as atrial predominant with highest abundance in purkinje fibers (qPCR, Taq-Man qPCR; Table 2) [5,10].

Reports of reduced *KCNK17* mRNA levels in atrial fibrillation [10] and heart failure [22,40] suggest a role for $K_{2P}17.1$ (TALK-2) in the pathophysiology of important cardiac pathologies. $K_{2P}17.1$ (TALK-2) channel subunits were described to heterodimerize with atrial $K_{2P}3.1$ (TASK-1), thereby modulating biophysical and pharmacological properties of atrial I_{TASK-1} [198]. In heterologous expressions systems, $K_{2P}17.1$ (TALK-2) channel homodimers were reported to be activated by propafenone, quinidine, mexiletine, propranolol, vernakalant, and metoprolol [75]. Amiodarone, sotalol, verapamil, and ranolazine were further described to inhibit $K_{2P}17.1$ (TALK-2) homodimers (Table 3) [75,83]. In iPSC, suppression of $K_{2P}17.1$ (TALK-2) expression was shown to prolong APD (Table 4) [22] while overexpression of $K_{2P}17.1$ (TALK-2) shortened APD levels in the cultured, cardiomyocyte derived HL-1 cell line [5]. Recently, a patient suffering from progressive and severe cardiac conduction disorder in combination with idiopathic ventricular fibrillation was identified to carry both, a splice site mutation in the sodium channel gene *SCN5A* as well as a mutation in the *KCNK17* gene [5]. This $K_{2P}17.1$ (TALK-2) G88R mutation, located in the first extracellular pore loop was shown to increase $K_{2P}17.1$ (TALK-2) currents to about three times upon heterologous expression. Overexpression of $K_{2P}17.1$ (TALK-2) G88R in spontaneously beating HL-1 cells was shown to result in a reduction of the beating frequency, hyperpolarization of the membrane potential and a strong slowing of the upstroke velocity [5].

Single nucleotide polymorphisms in the *KCNK17* gene which increase $K_{2P}17.1$ (TALK-2) channel subunit expression levels are associated with the occurrence of ischemic stroke in Caucasians but not in a Chinese population [137,199]. This observation links the channel once again to the pathophysiology of atrial fibrillation. *KCNK17* was further proposed as a genetic modifier of long QT syndrome type 2 severity, as a common *KCNK17* gain-of-function variant was shown to be LQTS protective by promoting APD shortening [74].

The cardiac characterization of the $K_{2P}17.1$ (TALK-2) channel is complicated by the fact that to date no specific inhibitors are available that would allow functional studies (Table 3). Furthermore, no ortholog to the *KCNK17* gene could be identified in mice and the porcine $K_{2P}17.1$ (TALK-2) channel subunit does not appear to show functional activity after heterologous expression in *Xenopus laevis* oocytes (unpublished observation of our lab).

17. $K_{2P}18.1$ (TRESK)

KCNK18 mRNA, encoding $K_{2P}18.1$ (TRESK) channel subunits was detected in human spinal cord, trigeminal ganglia, and brain but not in the heart (RT-PCR and TaqMan qPCR; Table 2) [10,61,77,78]. Accordingly, $K_{2P}18.1$ (TRESK) channels are supposed to play a key role in pain perception and *KCNK18* was identified as a potential susceptibility gene for migraine, while a cardiac role of this channel is rather unlikely [1]. TRESK channels may nevertheless exert indirect effects on the cardiovascular system: For example, high-fat diet-induced vagal afferent dysfunction has been described to be mediated via upregulation of $K_{2P}18.1$ (TRESK) [200]. Heterologously expressed $K_{2P}18.1$ (TRESK) channel homodimers are inhibited by lidocaine, verapamil, quinidine and apamin (Table 3) [76,200].

18. Conclusions

Overall, K_{2P} channels are an exciting and relevant new potassium channel class with relevance to a wide variety of disease conditions. For several members, reproducible mRNA regulation patterns in atrial fibrillation, heart failure and other cardiac disease could be described. However, the functional consequence remains difficult to assess, especially in cases where no specific channel inhibitors are available (Table 3), since surface expression and current amplitude in cardiomyocytes cannot be directly inferred from mRNA expression [11]. Further, the actual significance of the individual K_{2P} subgroups, some of which show only weak expression patterns, merits further investigation. To date, little is also known about the differential expression of K_{2P} channels in different cardiac cell populations and the consequence of remodelling in different cell types. In this regard, single cell next generation sequencing technology is expected to provide further evidence

soon. Furthermore, computational models of cardiac electrophysiology must consider effects of K$_{2P}$ channels. Taken together, emerging evidence suggests that K$_{2P}$ channels play an important role in cardiac repolarization and in the development of various cardiac arrhythmias such as atrial fibrillation, conduction disorders, and ventricular proarrhythmia that goes far beyond the role of unspecific leak currents.

References

1. Enyedi, P.; Czirják, G. Molecular Background of Leak K$^+$ Currents: Two-Pore Domain Potassium Channels. *Physiol. Rev.* **2010**, *90*, 559–605. [CrossRef] [PubMed]

2. Kraft, M.; Büscher, A.; Wiedmann, F.; L'hoste, Y.; Haefeli, W.E.; Frey, N.; Katus, H.A.; Schmidt, C. Current Drug Treatment Strategies for Atrial Fibrillation and TASK-1 Inhibition as an Emerging Novel Therapy Option. *Front. Pharm.* **2021**, *12*, 191. [CrossRef] [PubMed]

3. Schewe, M.; Nematian-Ardestani, E.; Sun, H.; Musinszki, M.; Cordeiro, S.; Bucci, G.; de Groot, B.L.; Tucker, S.J.; Rapedius, M.; Baukrowitz, T. A Non-canonical Voltage-Sensing Mechanism Controls Gating in K2P K(+) Channels. *Cell* **2016**, *164*, 937–949. [CrossRef] [PubMed]

4. Yue, D.T.; Marban, E. A novel cardiac potassium channel that is active and conductive at depolarized potentials. *Pflug. Arch.* **1988**, *413*, 127–133. [CrossRef]

5. Friedrich, C.; Rinné, S.; Zumhagen, S.; Kiper, A.K.; Silbernagel, N.; Netter, M.F.; Stallmeyer, B.; Schulze-Bahr, E.; Decher, N. Gain-of-function mutation in TASK-4 channels and severe cardiac conduction disorder. *EMBO Mol. Med.* **2014**, *6*, 937–951. [CrossRef]

6. Xu, H.; Guo, W.; Nerbonne, J.M. Four kinetically distinct depolarization-activated K+ currents in adult mouse ventricular myocytes. *J. Gen. Physiol.* **1999**, *113*, 661–678. [CrossRef]

7. Kim, D.; Clapham, D.E. Potassium channels in cardiac cells activated by arachidonic acid and phospholipids. *Science* **1989**, *244*, 1174–1176. [CrossRef]

8. Schmidt, C.; Wiedmann, F.; Voigt, N.; Zhou, X.B.; Heijman, J.; Lang, S.; Albert, V.; Kallenberger, S.; Ruhparwar, A.; Szabó, G.; et al. Upregulation of K(2P)3.1 K+ Current Causes Action Potential Shortening in Patients With Chronic Atrial Fibrillation. *Circulation* **2015**, *132*, 82–92. [CrossRef]

9. Renigunta, V.; Zou, X.; Kling, S.; Schlichthörl, G.; Daut, J. Breaking the silence: Functional expression of the two-pore-domain potassium channel THIK-2. *Pflug. Arch.* **2014**, *466*, 1735–1745. [CrossRef] [PubMed]

10. Christensen, A.H.; Chatelain, F.C.; Huttner, I.G.; Olesen, M.S.; Soka, M.; Feliciangeli, S.; Horvat, C.; Santiago, C.F.; Vandenberg, J.I.; Schmitt, N.; et al. The two-pore domain potassium channel, TWIK-1, has a role in the regulation of heart rate and atrial size. *J. Mol. Cell Cardiol.* **2016**, *97*, 24–35. [CrossRef]

11. Ellinghaus, P.; Scheubel, R.J.; Dobrev, D.; Ravens, U.; Holtz, J.; Huetter, J.; Nielsch, U.; Morawietz, H. Comparing the global mRNA expression profile of human atrial and ventricular myocardium with high-density oligonucleotide arrays. *J. Thorac. Cardiovasc. Surg.* **2005**, *129*, 1383–1390. [CrossRef]

12. Ördög, B.; Brutyó, E.; Puskás, L.G.; Papp, J.G.; Varró, A.; Szabad, J.; Boldogkői, Z. Gene expression profiling of human cardiac potassium and sodium channels. *Int. J. Cardiol.* **2006**, *111*, 386–393. [CrossRef]

13. Gaborit, N.; Le Bouter, S.; Szuts, V.; Varro, A.; Escande, D.; Nattel, S.; Demolombe, S. Regional and tissue specific transcript signatures of ion channel genes in the non-diseased human heart. *J. Physiol.* **2007**, *582*, 675–693. [CrossRef] [PubMed]

14. Putzke, C.; Wemhöner, K.; Sachse, F.B.; Rinné, S.; Schlichthörl, G.; Li, X.T.; Jaé, L.; Eckhardt, I.; Wischmeyer, E.; Wulf, H.; et al. The acid-sensitive potassium channel TASK-1 in rat cardiac muscle. *Cardiovasc. Res.* **2007**, *75*, 59–68. [CrossRef]

15. Wiedmann, F.; Schulte, J.S.; Gomes, B.; Zafeiriou, M.P.; Ratte, A.; Rathjens, F.; Fehrmann, E.; Scholz, B.; Voigt, N.; Müller, F.U.; et al. Atrial fibrillation and heart failure-associated remodeling of two-pore-domain potassium (K(2P)) channels in murine disease models: Focus on TASK-1. *Basic Res. Cardiol.* **2018**, *113*, 27. [CrossRef]

16. Howarth, F.C.; Qureshi, M.A.; Jayaprakash, P.; Parekh, K.; Oz, M.; Dobrzynski, H.; Adrian, T.E. The Pattern of mRNA Expression Is Changed in Sinoatrial Node from Goto-Kakizaki Type 2 Diabetic Rat Heart. *J. Diabetes Res.* **2018**, *2018*, 8454078. [CrossRef]

17. Liu, W.; Saint, D.A. Heterogeneous expression of tandem-pore K+ channel genes in adult and embryonic rat heart quantified by real-time polymerase chain reaction. *Clin. Exp. Pharm. Physiol.* **2004**, *31*, 174–178. [CrossRef] [PubMed]

18. Wang, Z.; Yue, L.; White, M.; Pelletier, G.; Nattel, S. Differential Distribution of Inward Rectifier Potassium Channel Transcripts in Human Atrium Versus Ventricle. *Circulation* **1998**, *98*, 2422–2428. [CrossRef] [PubMed]

19. McGeachie, M.; Ramoni, R.L.; Mychaleckyj, J.C.; Furie, K.L.; Dreyfuss, J.M.; Liu, Y.; Herrington, D.; Guo, X.; Lima, J.A.; Post, W.; et al. Integrative predictive model of coronary artery calcification in atherosclerosis. *Circulation* **2009**, *120*, 2448–2454. [CrossRef] [PubMed]

20. Schmidt, C.; Wiedmann, F.; Zhou, X.B.; Heijman, J.; Voigt, N.; Ratte, A.; Lang, S.; Kallenberger, S.M.; Campana, C.; Weymann, A.; et al. Inverse remodelling of K2P3.1 K+ channel expression and action potential duration in left ventricular dysfunction and atrial fibrillation: Implications for patient-specific antiarrhythmic drug therapy. *Eur. Heart J.* **2017**, *38*, 1764–1774. [CrossRef]

21. Chai, S.; Wan, X.; Nassal, D.M.; Liu, H.; Moravec, C.S.; Ramirez-Navarro, A.; Deschênes, I. Contribution of two-pore K(+) channels to cardiac ventricular action potential revealed using human iPSC-derived cardiomyocytes. *Am. J. Physiol. Heart Circ. Physiol.* **2017**, *312*, H1144–H1153. [CrossRef]

22. Medhurst, A.D.; Rennie, G.; Chapman, C.G.; Meadows, H.; Duckworth, M.D.; Kelsell, R.E.; Gloger, I.I.; Pangalos, M.N. Distribution analysis of human two pore domain potassium channels in tissues of the central nervous system and periphery. *Brain Res. Mol. Brain Res.* **2001**, *86*, 101–114. [CrossRef]

23. Fink, M.; Duprat, F.; Lesage, F.; Reyes, R.; Romey, G.; Heurteaux, C.; Lazdunski, M. Cloning, functional expression and brain localization of a novel unconventional outward rectifier K+ channel. *EMBO J.* **1996**, *15*, 6854–6862. [CrossRef]

24. Decher, N.; Wemhöner, K.; Rinné, S.; Netter, M.F.; Zuzarte, M.; Aller, M.I.; Kaufmann, S.G.; Li, X.T.; Meuth, S.G.; Daut, J.; et al. Knock-Out of the Potassium Channel TASK-1 Leads to a Prolonged QT Interval and a Disturbed QRS Complex. *Cell. Physiol. Biochem.* **2011**, *28*, 77–86. [CrossRef]

25. Donner, B.C.; Schullenberg, M.; Geduldig, N.; Hüning, A.; Mersmann, J.; Zacharowski, K.; Kovacevic, A.; Decking, U.; Aller, M.I.; Schmidt, K.G. Functional role of TASK-1 in the heart: Studies in TASK-1-deficient mice show prolonged cardiac repolarization and reduced heart rate variability. *Basic Res. Cardiol.* **2011**, *106*, 75–87. [CrossRef]

26. Hund, T.J.; Snyder, J.S.; Wu, X.; Glynn, P.; Koval, O.M.; Onal, B.; Leymaster, N.D.; Unudurthi, S.D.; Curran, J.; Camardo, C.; et al. βIV-Spectrin regulates TREK-1 membrane targeting in the heart. *Cardiovasc. Res.* **2014**, *102*, 166–175. [CrossRef] [PubMed]

27. Aimond, F.; Rauzier, J.-M.; Bony, C.; Vassort, G. Simultaneous Activation of p38 MAPK and p42/44 MAPK by ATP Stimulates the K+ Current ITREK in Cardiomyocytes. *J. Biol. Chem.* **2000**, *275*, 39110–39116. [CrossRef] [PubMed]

28. Tan, J.H.; Liu, W.; Saint, D.A. Trek-like potassium channels in rat cardiac ventricular myocytes are activated by intracellular ATP. *J. Membr. Biol.* **2002**, *185*, 201–207. [CrossRef] [PubMed]

29. Tan, J.H.C.; Liu, W.; Saint, D.A. Differential expression of the mechanosensitive potassium channel TREK-1 in epicardial and endocardial myocytes in rat ventricle. *Exp. Physiol.* **2004**, *89*, 237–242. [CrossRef]

30. Rinné, S.; Renigunta, V.; Schlichthörl, G.; Zuzarte, M.; Bittner, S.; Meuth, S.G.; Decher, N.; Daut, J.; Preisig-Müller, R. A splice variant of the two-pore domain potassium channel TREK-1 with only one pore domain reduces the surface expression of full-length TREK-1 channels. *Pflug. Arch.* **2014**, *466*, 1559–1570. [CrossRef]

31. Terrenoire, C.; Lauritzen, I.; Lesage, F.; Romey, G.; Lazdunski, M. A TREK-1–Like Potassium Channel in Atrial Cells Inhibited by β-Adrenergic Stimulation and Activated by Volatile Anesthetics. *Circ. Res.* **2001**, *89*, 336–342. [CrossRef] [PubMed]

32. Li, X.T.; Dyachenko, V.; Zuzarte, M.; Putzke, C.; Preisig-Müller, R.; Isenberg, G.; Daut, J. The stretch-activated potassium channel TREK-1 in rat cardiac ventricular muscle. *Cardiovasc. Res.* **2006**, *69*, 86–97. [CrossRef]

33. Jones, S.A.; Morton, M.J.; Hunter, M.; Boyett, M.R. Expression of TASK-1, a pH-sensitive twin-pore domain K(+) channel, in rat myocytes. *Am. J. Physiol. Heart Circ. Physiol.* **2002**, *283*, H181–H185. [CrossRef]

34. Schmidt, C.; Wiedmann, F.; Tristram, F.; Anand, P.; Wenzel, W.; Lugenbiel, P.; Schweizer, P.A.; Katus, H.A.; Thomas, D. Cardiac expression and atrial fibrillation-associated remodeling of K2P2.1 (TREK-1) K+ channels in a porcine model. *Life Sci.* **2014**, *97*, 107–115. [CrossRef]

35. Lugenbiel, P.; Wenz, F.; Syren, P.; Geschwill, P.; Govorov, K.; Seyler, C.; Frank, D.; Schweizer, P.A.; Franke, J.; Weis, T.; et al. TREK-1 (K(2P)2.1) K(+) channels are suppressed in patients with atrial fibrillation and heart failure and provide therapeutic targets for rhythm control. *Basic Res. Cardiol.* **2017**, *112*, 8. [CrossRef] [PubMed]

36. Marionneau, C.; Aimond, F.; Brunet, S.; Niwa, N.; Finck, B.; Kelly, D.P.; Nerbonne, J.M. PPARalpha-mediated remodeling of repolarizing voltage-gated K+ (Kv) channels in a mouse model of metabolic cardiomyopathy. *J. Mol. Cell. Cardiol.* **2008**, *44*, 1002–1015. [CrossRef]

37. Limberg, S.H.; Netter, M.F.; Rolfes, C.; Rinné, S.; Schlichthörl, G.; Zuzarte, M.; Vassiliou, T.; Moosdorf, R.; Wulf, H.; Daut, J.; et al. TASK-1 channels may modulate action potential duration of human atrial cardiomyocytes. *Cell Physiol. Biochem.* **2011**, *28*, 613–624. [CrossRef] [PubMed]

38. Schmidt, C.; Wiedmann, F.; Kallenberger, S.M.; Ratte, A.; Schulte, J.S.; Scholz, B.; Müller, F.U.; Voigt, N.; Zafeiriou, M.-P.; Ehrlich, J.R.; et al. Stretch-activated two-pore-domain (K2P) potassium channels in the heart: Focus on atrial fibrillation and heart failure. *Prog. Biophys. Mol. Biol.* **2017**, *130*, 233–243. [CrossRef] [PubMed]

39. Staudacher, K.; Staudacher, I.; Ficker, E.; Seyler, C.; Gierten, J.; Kisselbach, J.; Rahm, A.K.; Trappe, K.; Schweizer, P.A.; Becker, R.; et al. Carvedilol targets human K2P 3.1 (TASK1) K+ leak channels. *Br. J. Pharm.* **2011**, *163*, 1099–1110. [CrossRef]

40. Gaborit, N.; Wichter, T.; Varro, A.; Szuts, V.; Lamirault, G.; Eckardt, L.; Paul, M.; Breithardt, G.; Schulze-Bahr, E.; Escande, D.; et al. Transcriptional profiling of ion channel genes in Brugada syndrome and other right ventricular arrhythmogenic diseases. *Eur. Heart J.* **2009**, *30*, 487–496. [CrossRef] [PubMed]

41. Kisselbach, J.; Seyler, C.; Schweizer, P.A.; Gerstberger, R.; Becker, R.; Katus, H.A.; Thomas, D. Modulation of K2P 2.1 and K2P 10.1 K(+) channel sensitivity to carvedilol by alternative mRNA translation initiation. *Br. J. Pharm.* **2014**, *171*, 5182–5194. [CrossRef]

42. Graham, V.; Zhang, H.; Willis, S.; Creazzo, T.L. Expression of a two-pore domain K+ channel (TASK-1) in developing avian and mouse ventricular conduction systems. *Dev. Dyn.* **2006**, *235*, 143–151. [CrossRef] [PubMed]

43. Duprat, F.; Lesage, F.; Fink, M.; Reyes, R.; Heurteaux, C.; Lazdunski, M. TASK, a human background K+ channel to sense external pH variations near physiological pH. *EMBO J.* **1997**, *16*, 5464–5471. [CrossRef]

44. Duan, W.; Hicks, J.; Makara, M.A.; Ilkayeva, O.; Abraham, D.M. TASK-1 and TASK-3 channels modulate pressure overload-induced cardiac remodeling and dysfunction. *Am. J. Physiol. Heart Circ. Physiol.* **2020**, *318*, H566–H580. [CrossRef]

45. Kim, Y.; Bang, H.; Kim, D. TBAK-1 and TASK-1, two-pore K(+) channel subunits: Kinetic properties and expression in rat heart. *Am. J. Physiol.* **1999**, *277*, H1669–H1678. [CrossRef]

46. Karschin, C.; Wischmeyer, E.; Preisig-Müller, R.; Rajan, S.; Derst, C.; Grzeschik, K.H.; Daut, J.; Karschin, A. Expression pattern in brain of TASK-1, TASK-3, and a tandem pore domain K(+) channel subunit, TASK-5, associated with the central auditory nervous system. *Mol. Cell Neurosci.* **2001**, *18*, 632–648. [CrossRef]

47. Skarsfeldt, M.A.; Jepps, T.A.; Bomholtz, S.H.; Abildgaard, L.; Sørensen, U.S.; Gregers, E.; Svendsen, J.H.; Diness, J.G.; Grunnet, M.; Schmitt, N.; et al. pH-dependent inhibition of $K_2P3.1$ prolongs atrial refractoriness in whole hearts. *Pflug. Arch.* **2016**, *468*, 643–654. [CrossRef]

48. Harleton, E.; Besana, A.; Comas, G.M.; Danilo, P.; Rosen, T.S.; Argenziano, M.; Rosen, M.R.; Robinson, R.B.; Feinmark, S.J. Ability to Induce Atrial Fibrillation in the Peri-operative Period Is Associated with Phosphorylation-dependent Inhibition of TWIK Protein-related Acid-sensitive Potassium Channel 1 (TASK-1)*. *J. Biol. Chem.* **2013**, *288*, 2829–2838. [CrossRef] [PubMed]

49. Schmidt, C.; Wiedmann, F.; Langer, C.; Tristram, F.; Anand, P.; Wenzel, W.; Lugenbiel, P.; Schweizer, P.A.; Katus, H.A.; Thomas, D. Cloning, functional characterization, and remodeling of K2P3.1 (TASK-1) potassium channels in a porcine model of atrial fibrillation and heart failure. *Heart Rhythm* **2014**, *11*, 1798–1805. [CrossRef] [PubMed]

50. Schmidt, C.; Wiedmann, F.; Beyersdorf, C.; Zhao, Z.; El-Battrawy, I.; Lan, H.; Szabo, G.; Li, X.; Lang, S.; Korkmaz-Icöz, S.; et al. Genetic Ablation of TASK-1 (Tandem of P Domains in a Weak Inward Rectifying K(+) Channel-Related Acid-Sensitive K(+) Channel-1) (K(2P)3.1) K(+) Channels Suppresses Atrial Fibrillation and Prevents Electrical Remodeling. *Circ. Arrhythm. Electrophysiol.* **2019**, *12*, e007465. [CrossRef]

51. Wiedmann, F.; Beyersdorf, C.; Zhou, X.B.; Kraft, M.; Paasche, A.; Jávorszky, N.; Rinné, S.; Sutanto, H.; Büscher, A.; Foerster, K.I.; et al. Treatment of atrial fibrillation with doxapram: TASK-1 potassium channel inhibition as a novel pharmacological strategy. *Cardiovasc. Res.* **2021**. [CrossRef] [PubMed]

52. Wiedmann, F.; Beyersdorf, C.; Zhou, X.; Büscher, A.; Kraft, M.; Nietfeld, J.; Walz, T.P.; Unger, L.A.; Loewe, A.; Schmack, B.; et al. Pharmacologic TWIK-Related Acid-Sensitive K+ Channel (TASK-1) Potassium Channel Inhibitor A293 Facilitates Acute Cardioversion of Paroxysmal Atrial Fibrillation in a Porcine Large Animal Model. *J. Am. Heart Assoc.* **2020**, *9*, e015751. [CrossRef] [PubMed]

53. Barth, A.S.; Merk, S.; Arnoldi, E.; Zwermann, L.; Kloos, P.; Gebauer, M.; Steinmeyer, K.; Bleich, M.; Kääb, S.; Hinterseer, M.; et al. Reprogramming of the human atrial transcriptome in permanent atrial fibrillation: Expression of a ventricular-like genomic signature. *Circ. Res.* **2005**, *96*, 1022–1029. [CrossRef] [PubMed]

54. Rinné, S.; Kiper, A.K.; Schlichthörl, G.; Dittmann, S.; Netter, M.F.; Limberg, S.H.; Silbernagel, N.; Zuzarte, M.; Moosdorf, R.; Wulf, H.; et al. TASK-1 and TASK-3 may form heterodimers in human atrial cardiomyocytes. *J. Mol. Cell Cardiol.* **2015**, *81*, 71–80. [CrossRef]

55. Darkow, E.; Nguyen, T.T.; Stolina, M.; Kari, F.A.; Schmidt, C.; Wiedmann, F.; Baczkó, I.; Kohl, P.; Rajamani, S.; Ravens, U.; et al. Small Conductance Ca(2 +)-Activated K(+) (SK) Channel mRNA Expression in Human Atrial and Ventricular Tissue: Comparison Between Donor, Atrial Fibrillation and Heart Failure Tissue. *Front. Physiol.* **2021**, *12*, 650964. [CrossRef]

56. Fink, M.; Lesage, F.; Duprat, F.; Heurteaux, C.; Reyes, R.; Fosset, M.; Lazdunski, M. A neuronal two P domain K+ channel stimulated by arachidonic acid and polyunsaturated fatty acids. *EMBO J.* **1998**, *17*, 3297–3308. [CrossRef]

57. Meadows, H.J.; Chapman, C.G.; Duckworth, D.M.; Kelsell, R.E.; Murdock, P.R.; Nasir, S.; Rennie, G.; Randall, A.D. The neuroprotective agent sipatrigine (BW619C89) potently inhibits the human tandem pore-domain K(+) channels TREK-1 and TRAAK. *Brain Res.* **2001**, *892*, 94–101. [CrossRef]

58. Kang, D.; Kim, D. Single-channel properties and pH sensitivity of two-pore domain K+ channels of the TALK family. *Biochem. Biophys. Res. Commun.* **2004**, *315*, 836–844. [CrossRef]

59. Liu, C.; Au, J.D.; Zou, H.L.; Cotten, J.F.; Yost, C.S. Potent activation of the human tandem pore domain K channel TRESK with clinical concentrations of volatile anesthetics. *Anesth. Analg.* **2004**, *99*, 1715–1722. [CrossRef]

60. Patel, A.J.; Maingret, F.; Magnone, V.; Fosset, M.; Lazdunski, M.; Honoré, E. TWIK-2, an inactivating 2P domain K+ channel. *J. Biol. Chem.* **2000**, *275*, 28722–28730. [CrossRef]

61. Wang, R.P.; Wang, S.; Chen, D.; Yang, N.; Lei, L.C.; Wang, Z.Y.; Ye, H.M.; Ren, L.H.; Yang, S.X. mRNA genomics change and significance of important ion channel proteins in patients with atrial fibrillation. *Zhonghua Yi Xue Za Zhi* **2018**, *98*, 3171–3177. [CrossRef] [PubMed]

62. Rajan, S.; Wischmeyer, E.; Liu, G.X.; Preisig-Müller, R.; Daut, J.; Karschin, A.; Derst, C. TASK-3, a novel tandem pore domain acid-sensitive K+ channel. An extracellular histidin as pH sensor. *J. Biol. Chem.* **2000**, *275*, 16650–16657. [CrossRef]

63. Bang, H.; Kim, Y.; Kim, D. TREK-2, a new member of the mechanosensitive tandem-pore K+ channel family. *J. Biol. Chem.* **2000**, *275*, 17412–17419. [CrossRef] [PubMed]

64. Rajan, S.; Wischmeyer, E.; Karschin, C.; Preisig-Müller, R.; Grzeschik, K.H.; Daut, J.; Karschin, A.; Derst, C. THIK-1 and THIK-2, a novel subfamily of tandem pore domain K+ channels. *J. Biol. Chem.* **2001**, *276*, 7302–7311. [CrossRef]

65. Girard, C.; Duprat, F.; Terrenoire, C.; Tinel, N.; Fosset, M.; Romey, G.; Lazdunski, M.; Lesage, F. Genomic and Functional Characteristics of Novel Human Pancreatic 2P Domain K+ Channels. *Biochem. Biophys. Res. Commun.* **2001**, *282*, 249–256. [CrossRef]

66. Staudacher, I.; Seehausen, S.; Gierten, J.; Illg, C.; Schweizer, P.A.; Katus, H.A.; Thomas, D. Cloning and characterization of zebrafish K(2P)13.1 (THIK-1) two-pore-domain K(+) channels. *J. Mol. Cell Cardiol.* **2019**, *126*, 96–104. [CrossRef] [PubMed]

67. Ashmole, I.; Goodwin, P.A.; Stanfield, P.R. TASK-5, a novel member of the tandem pore K+ channel family. *Pflügers Arch.* **2001**, *442*, 828–833. [CrossRef]

68. Kim, D.; Gnatenco, C. TASK-5, a new member of the tandem-pore K(+) channel family. *Biochem. Biophys. Res. Commun.* **2001**, *284*, 923–930. [CrossRef]

69. Han, J.; Kang, D.; Kim, D. Functional properties of four splice variants of a human pancreatic tandem-pore K+ channel, TALK-1. *Am. J. Physiol. Cell Physiol.* **2003**, *285*, C529–C538. [CrossRef] [PubMed]

70. Staudacher, I.; Illg, C.; Gierten, J.; Seehausen, S.; Schweizer, P.A.; Katus, H.A.; Thomas, D. Identification and functional characterization of zebrafish K(2P)17.1 (TASK-4, TALK-2) two-pore-domain K(+) channels. *Eur. J. Pharm.* **2018**, *831*, 94–102. [CrossRef]

71. Decher, N.; Maier, M.; Dittrich, W.; Gassenhuber, J.; Brüggemann, A.; Busch, A.E.; Steinmeyer, K. Characterization of TASK-4, a novel member of the pH-sensitive, two-pore domain potassium channel family. *FEBS Lett.* **2001**, *492*, 84–89. [CrossRef]

72. Chai, S.; Wan, X.; Ramirez-Navarro, A.; Tesar, P.J.; Kaufman, E.S.; Ficker, E.; George, A.L., Jr.; Deschênes, I. Physiological genomics identifies genetic modifiers of long QT syndrome type 2 severity. *J. Clin. Invest.* **2018**, *128*, 1043–1056. [CrossRef]

73. Staudacher, I.; Illg, C.; Chai, S.; Deschenes, I.; Seehausen, S.; Gramlich, D.; Müller, M.E.; Wieder, T.; Rahm, A.K.; Mayer, C.; et al. Cardiovascular pharmacology of K(2P)17.1 (TASK-4, TALK-2) two-pore-domain K(+) channels. *Naunyn Schmiedebergs Arch. Pharm.* **2018**, *391*, 1119–1131. [CrossRef] [PubMed]

74. Rahm, A.K.; Wiedmann, F.; Gierten, J.; Schmidt, C.; Schweizer, P.A.; Becker, R.; Katus, H.A.; Thomas, D. Functional character-ization of zebrafish K2P18.1 (TRESK) two-pore-domain K+ channels. *Naunyn Schmiedebergs Arch. Pharm.* **2014**, *387*, 291–300. [CrossRef]

75. Keshavaprasad, B.; Liu, C.; Au, J.D.; Kindler, C.H.; Cotten, J.F.; Yost, C.S. Species-specific differences in response to anesthetics and other modulators by the K2P channel TRESK. *Anesth. Analg.* **2005**, *101*, 1042–1049. [CrossRef]

76. Sano, Y.; Inamura, K.; Miyake, A.; Mochizuki, S.; Kitada, C.; Yokoi, H.; Nozawa, K.; Okada, H.; Matsushime, H.; Furuichi, K. A novel two-pore domain K+ channel, TRESK, is localized in the spinal cord. *J. Biol. Chem.* **2003**, *278*, 27406–27412. [CrossRef]

77. Wiedmann, F.; Rinné, S.; Donner, B.; Decher, N.; Katus, H.A.; Schmidt, C. Mechanosensitive TREK-1 two-pore-domain potassium (K(2P)) channels in the cardiovascular system. *Prog. Biophys. Mol. Biol.* **2021**, *159*, 126–135. [CrossRef] [PubMed]

78. Wiedmann, F.; Schlund, D.; Faustino, F.; Kraft, M.; Ratte, A.; Thomas, D.; Katus, H.A.; Schmidt, C. N-Glycosylation of TREK-1/hK(2P)2.1 Two-Pore-Domain Potassium (K(2P)) Channels. *Int. J. Mol. Sci.* **2019**, *20*, 5193. [CrossRef]

79. Lesage, F.; Guillemare, E.; Fink, M.; Duprat, F.; Lazdunski, M.; Romey, G.; Barhanin, J. TWIK-1, a ubiquitous human weakly inward rectifying K+ channel with a novel structure. *EMBO J.* **1996**, *15*, 1004–1011. [CrossRef]

80. Gaborit, N.; Steenman, M.; Lamirault, G.; Le Meur, N.; Le Bouter, S.; Lande, G.; Léger, J.; Charpentier, F.; Christ, T.; Dobrev, D.; et al. Human atrial ion channel and transporter subunit gene-expression remodeling associated with valvular heart disease and atrial fibrillation. *Circulation* **2005**, *112*, 471–481. [CrossRef] [PubMed]

81. Schmidt, C.; Wiedmann, F.; Schweizer, P.A.; Becker, R.; Katus, H.A.; Thomas, D. Novel electrophysiological properties of dronedarone: Inhibition of human cardiac two-pore-domain potassium (K2P) channels. *Naunyn Schmiedebergs Arch. Pharm.* **2012**, *385*, 1003–1016. [CrossRef]

82. Lesage, F.; Lazdunski, M. Molecular and functional properties of two-pore-domain potassium channels. *Am. J. Physiol. Ren. Physiol.* **2000**, *279*, F793–F801. [CrossRef]

83. Loucif, A.J.C.; Saintot, P.P.; Liu, J.; Antonio, B.M.; Zellmer, S.G.; Yoger, K.; Veale, E.L.; Wilbrey, A.; Omoto, K.; Cao, L.; et al. GI-530159, a novel, selective, mechanosensitive two-pore-domain potassium (K(2P)) channel opener, reduces rat dorsal root ganglion neuron excitability. *Br. J. Pharm.* **2018**, *175*, 2272–2283. [CrossRef] [PubMed]

84. Goonetilleke, L.; Quayle, J. TREK-1 K(+) channels in the cardiovascular system: Their significance and potential as a therapeutic target. *Cardiovasc. Ther.* **2012**, *30*, e23–e29. [CrossRef]

85. Gruss, M.; Mathie, A.; Lieb, W.R.; Franks, N.P. The two-pore-domain K(+) channels TREK-1 and TASK-3 are differentially modulated by copper and zinc. *Mol. Pharm.* **2004**, *66*, 530–537. [CrossRef]

86. Joseph, A.; Thuy, T.T.T.; Thanh, L.T.; Okada, M. Antidepressive and anxiolytic effects of ostruthin, a TREK-1 channel activator. *PLoS ONE* **2018**, *13*, e0201092. [CrossRef]

87. Pope, L.; Arrigoni, C.; Lou, H.; Bryant, C.; Gallardo-Godoy, A.; Renslo, A.R.; Minor, D.L., Jr. Protein and Chemical Determinants of BL-1249 Action and Selectivity for K(2P) Channels. *ACS Chem. Neurosci.* **2018**, *9*, 3153–3165. [CrossRef]

88. Lolicato, M.; Arrigoni, C.; Mori, T.; Sekioka, Y.; Bryant, C.; Clark, K.A.; Minor, D.L., Jr. K(2P)2.1 (TREK-1)-activator complexes reveal a cryptic selectivity filter binding site. *Nature* **2017**, *547*, 364–368. [CrossRef]

89. Bagriantsev, S.N.; Ang, K.H.; Gallardo-Godoy, A.; Clark, K.A.; Arkin, M.R.; Renslo, A.R.; Minor, D.L., Jr. A high-throughput functional screen identifies small molecule regulators of temperature- and mechano-sensitive K2P channels. *ACS Chem. Biol.* **2013**, *8*, 1841–1851. [CrossRef] [PubMed]

90. Wright, P.D.; McCoull, D.; Walsh, Y.; Large, J.M.; Hadrys, B.W.; Gaurilcikaite, E.; Byrom, L.; Veale, E.L.; Jerman, J.; Mathie, A. Pranlukast is a novel small molecule activator of the two-pore domain potassium channel TREK2. *Biochem. Biophys. Res. Commun.* **2019**, *520*, 35–40. [CrossRef]

91. Minieri, L.; Pivonkova, H.; Caprini, M.; Harantova, L.; Anderova, M.; Ferroni, S. The inhibitor of volume-regulated anion channels DCPIB activates TREK potassium channels in cultured astrocytes. *Br. J. Pharm.* **2013**, *168*, 1240–1254. [CrossRef]

92. Devilliers, M.; Busserolles, J.; Lolignier, S.; Deval, E.; Pereira, V.; Alloui, A.; Christin, M.; Mazet, B.; Delmas, P.; Noel, J.; et al. Activation of TREK-1 by morphine results in analgesia without adverse side effects. *Nat. Commun.* **2013**, *4*, 2941. [CrossRef]

93. Takahira, M.; Sakurai, M.; Sakurada, N.; Sugiyama, K. Fenamates and diltiazem modulate lipid-sensitive mechano-gated 2P domain K(+) channels. *Pflug. Arch.* **2005**, *451*, 474–478. [CrossRef] [PubMed]

94. Gruss, M.; Bushell, T.J.; Bright, D.P.; Lieb, W.R.; Mathie, A.; Franks, N.P. Two-pore-domain K+ channels are a novel target for the anesthetic gases xenon, nitrous oxide, and cyclopropane. *Mol. Pharm.* **2004**, *65*, 443–452. [CrossRef]

95. Mazella, J.; Pétrault, O.; Lucas, G.; Deval, E.; Béraud-Dufour, S.; Gandin, C.; El-Yacoubi, M.; Widmann, C.; Guyon, A.; Chevet, E.; et al. Spadin, a sortilin-derived peptide, targeting rodent TREK-1 channels: A new concept in the antidepressant drug design. *PLoS Biol.* **2010**, *8*, e1000355. [CrossRef] [PubMed]

96. Unudurthi, S.D.; Wu, X.; Qian, L.; Amari, F.; Onal, B.; Li, N.; Makara, M.A.; Smith, S.A.; Snyder, J.; Fedorov, V.V.; et al. Two-Pore K+ Channel TREK-1 Regulates Sinoatrial Node Membrane Excitability. *J. Am. Heart Assoc.* **2016**, *5*, e002865. [CrossRef]

97. Thomas, D.; Plant, L.D.; Wilkens, C.M.; McCrossan, Z.A.; Goldstein, S.A.N. Alternative Translation Initiation in Rat Brain Yields K2P2.1 Potassium Channels Permeable to Sodium. *Neuron* **2008**, *58*, 859–870. [CrossRef]

98. Liu, H.; Enyeart, J.A.; Enyeart, J.J. Potent Inhibition of Native TREK-1 K+ Channels by Selected Dihydropyridine Ca^{2+} Channel Antagonists. *J. Pharmacol. Exp. Ther.* **2007**, *323*, 39–48. [CrossRef]

99. Streit, A.K.; Netter, M.F.; Kempf, F.; Walecki, M.; Rinné, S.; Bollepalli, M.K.; Preisig-Müller, R.; Renigunta, V.; Daut, J.; Baukrowitz, T.; et al. A specific two-pore domain potassium channel blocker defines the structure of the TASK-1 open pore. *J. Biol. Chem.* **2011**, *286*, 13977–13984. [CrossRef]

100. Shin, H.W.; Soh, J.S.; Kim, H.Z.; Hong, J.; Woo, D.H.; Heo, J.Y.; Hwang, E.M.; Park, J.Y.; Lee, C.J. The inhibitory effects of bupivacaine, levobupivacaine, and ropivacaine on K2P (two-pore domain potassium) channel TREK-1. *J. Anesth.* **2014**, *28*, 81–86. [CrossRef] [PubMed]

101. Ratte, A.; Wiedmann, F.; Kraft, M.; Katus, H.A.; Schmidt, C. Antiarrhythmic Properties of Ranolazine: Inhibition of Atrial Fibrillation Associated TASK-1 Potassium Channels. *Front. Pharm.* **2019**, *10*, 1367. [CrossRef]

102. Thümmler, S.; Duprat, F.; Lazdunski, M. Antipsychotics inhibit TREK but not TRAAK channels. *Biochem. Biophys. Res. Commun.* **2007**, *354*, 284–289. [CrossRef] [PubMed]

103. Punke, M.A.; Licher, T.; Pongs, O.; Friederich, P. Inhibition of human TREK-1 channels by bupivacaine. *Anesth. Analg.* **2003**, *96*, 1665–1673. [CrossRef]

104. Nayak, T.K.; Harinath, S.; Nama, S.; Somasundaram, K.; Sikdar, S.K. Inhibition of Human Two-Pore Domain K+ Channel TREK1 by Local Anesthetic Lidocaine: Negative Cooperativity and Half-of-Sites Saturation Kinetics. *Mol. Pharmacol.* **2009**, *76*, 903–917. [CrossRef]

105. Harinath, S.; Sikdar, S.K. Inhibition of human TREK-1 channels by caffeine and theophylline. *Epilepsy Res.* **2005**, *64*, 127–135. [CrossRef]

106. Zhang, H.; Shepherd, N.; Creazzo, T.L. Temperature-sensitive TREK currents contribute to setting the resting membrane potential in embryonic atrial myocytes. *J. Physiol.* **2008**, *586*, 3645–3656. [CrossRef]

107. Gierten, J.; Ficker, E.; Bloehs, R.; Schweizer, P.A.; Zitron, E.; Scholz, E.; Karle, C.; Katus, H.A.; Thomas, D. The human cardiac K2P3.1 (TASK-1) potassium leak channel is a molecular target for the class III antiarrhythmic drug amiodarone. *Naunyn Schmiedebergs Arch. Pharm.* **2010**, *381*, 261–270. [CrossRef] [PubMed]

108. Schmidt, C.; Wiedmann, F.; Gaubatz, A.R.; Ratte, A.; Katus, H.A.; Thomas, D. New Targets for Old Drugs: Cardiac Glycosides Inhibit Atrial-Specific K(2P)3.1 (TASK-1) Channels. *J. Pharm. Exp.* **2018**, *365*, 614–623. [CrossRef]

109. Seyler, C.; Li, J.; Schweizer, P.A.; Katus, H.A.; Thomas, D. Inhibition of cardiac two-pore-domain K+ (K2P) channels by the antiarrhythmic drug vernakalant–comparison with flecainide. *Eur. J. Pharm.* **2014**, *724*, 51–57. [CrossRef]

110. Bae, C.; Sachs, F.; Gottlieb, P.A. The mechanosensitive ion channel Piezo1 is inhibited by the peptide GsMTx4. *Biochemistry* **2011**, *50*, 6295–6300. [CrossRef] [PubMed]

111. Putzke, C.; Hanley, P.J.; Schlichthörl, G.; Preisig-Müller, R.; Rinné, S.; Anetseder, M.; Eckenhoff, R.; Berkowitz, C.; Vassiliou, T.; Wulf, H.; et al. Differential effects of volatile and intravenous anesthetics on the activity of human TASK-1. *Am. J. Physiol. Cell Physiol.* **2007**, *293*, C1319–C1326. [CrossRef] [PubMed]

112. Sirois, J.E.; Lei, Q.; Talley, E.M.; Lynch, C., 3rd; Bayliss, D.A. The TASK-1 two-pore domain K+ channel is a molecular substrate for neuronal effects of inhalation anesthetics. *J. Neurosci.* **2000**, *20*, 6347–6354. [CrossRef] [PubMed]

113. Rödström, K.E.J.; Kiper, A.K.; Zhang, W.; Rinné, S.; Pike, A.C.W.; Goldstein, M.; Conrad, L.J.; Delbeck, M.; Hahn, M.G.; Meier, H.; et al. A lower X-gate in TASK channels traps inhibitors within the vestibule. *Nature* **2020**, *582*, 443–447. [CrossRef] [PubMed]

114. Zou, B.; Flaherty, D.P.; Simpson, D.S.; Maki, B.E.; Miller, M.R.; Shi, J.; Wu, M.; McManus, O.B.; Golden, J.E.; Aubé, J.; et al. ML365: Development of Bis-Amides as Selective Inhibitors of the KCNK3/TASK1 Two Pore Potassium Channel. In *Probe Reports from the NIH Molecular Libraries Program*; National Center for Biotechnology Information (US): Bethesda, MD, USA, 2010.

115. Kiper, A.K.; Rinné, S.; Rolfes, C.; Ramírez, D.; Seebohm, G.; Netter, M.F.; González, W.; Decher, N. Kv1.5 blockers preferentially inhibit TASK-1 channels: TASK-1 as a target against atrial fibrillation and obstructive sleep apnea? *Pflug. Arch.* **2015**, *467*, 1081–1090. [CrossRef]

116. Ramírez, D.; Bedoya, M.; Kiper, A.K.; Rinné, S.; Morales-Navarro, S.; Hernández-Rodríguez, E.W.; Sepúlveda, F.V.; Decher, N.; González, W. Structure/Activity Analysis of TASK-3 Channel Antagonists Based on a 5,6,7,8 tetrahydropyrido[4, 3-d]pyrimidine. *Int. J. Mol. Sci.* **2019**, *20*, 2252. [CrossRef] [PubMed]

117. Cotten, J.F.; Keshavaprasad, B.; Laster, M.J.; Eger, E.I., 2nd; Yost, C.S. The ventilatory stimulant doxapram inhibits TASK tandem pore (K2P) potassium channel function but does not affect minimum alveolar anesthetic concentration. *Anesth. Analg.* **2006**, *102*, 779–785. [CrossRef] [PubMed]

118. Maingret, F.; Patel, A.J.; Lazdunski, M.; Honoré, E. The endocannabinoid anandamide is a direct and selective blocker of the background K(+) channel TASK-1. *EMBO J.* **2001**, *20*, 47–54. [CrossRef] [PubMed]

119. Miller, M.R.; Zou, B.; Shi, J.; Flaherty, D.P.; Simpson, D.S.; Yao, T.; Maki, B.E.; Day, V.W.; Douglas, J.T.; Wu, M.; et al. Development of a Selective Chemical Inhibitor for the Two-Pore Potassium Channel, KCNK9. In *Probe Reports from the NIH Molecular Libraries Program*; National Center for Biotechnology Information (US): Bethesda, MD, USA, 2010.

120. Kindler, C.H.; Yost, C.S.; Gray, A.T. Local anesthetic inhibition of baseline potassium channels with two pore domains in tandem. *Anesthesiology* **1999**, *90*, 1092–1102. [CrossRef] [PubMed]

121. Leonoudakis, D.; Gray, A.T.; Winegar, B.D.; Kindler, C.H.; Harada, M.; Taylor, D.M.; Chavez, R.A.; Forsayeth, J.R.; Yost, C.S. An open rectifier potassium channel with two pore domains in tandem cloned from rat cerebellum. *J. Neurosci.* **1998**, *18*, 868–877. [CrossRef] [PubMed]

122. Meadows, H.J.; Randall, A.D. Functional characterisation of human TASK-3, an acid-sensitive two-pore domain potassium channel. *Neuropharmacology* **2001**, *40*, 551–559. [CrossRef]

123. Bruner, J.K.; Zou, B.; Zhang, H.; Zhang, Y.; Schmidt, K.; Li, M. Identification of novel small molecule modulators of K2P18.1 two-pore potassium channel. *Eur. J. Pharmacol.* **2014**, *740*, 603–610. [CrossRef]

124. Eckert, M.; Egenberger, B.; Döring, F.; Wischmeyer, E. TREK-1 isoforms generated by alternative translation initiation display different susceptibility to the antidepressant fluoxetine. *Neuropharmacology* **2011**, *61*, 918–923. [CrossRef]

125. Braun, G.; Lengyel, M.; Enyedi, P.; Czirják, G. Differential sensitivity of TREK-1, TREK-2 and TRAAK background potassium channels to the polycationic dye ruthenium red. *Br. J. Pharm.* **2015**, *172*, 1728–1738. [CrossRef]

126. Dadi, P.K.; Vierra, N.C.; Days, E.; Dickerson, M.T.; Vinson, P.N.; Weaver, C.D.; Jacobson, D.A. Selective Small Molecule Activators of TREK-2 Channels Stimulate Dorsal Root Ganglion c-Fiber Nociceptor Two-Pore-Domain Potassium Channel Currents and Limit Calcium Influx. *ACS Chem. Neurosci.* **2017**, *8*, 558–568. [CrossRef] [PubMed]

127. Staudacher, I.; Seehausen, S.; Illg, C.; Lugenbiel, P.; Schweizer, P.A.; Katus, H.A.; Thomas, D. Cardiac K(2P)13.1 (THIK-1) two-pore-domain K(+) channels: Pharmacological regulation and remodeling in atrial fibrillation. *Prog. Biophys. Mol. Biol.* **2019**, *144*, 128–138. [CrossRef]

128. Wright, P.D.; Weir, G.; Cartland, J.; Tickle, D.; Kettleborough, C.; Cader, M.Z.; Jerman, J. Cloxyquin (5-chloroquinolin-8-ol) is an activator of the two-pore domain potassium channel TRESK. *Biochem. Biophys. Res. Commun.* **2013**, *441*, 463–468. [CrossRef] [PubMed]

129. Czirják, G.; Enyedi, P. Zinc and Mercuric Ions Distinguish TRESK from the Other Two-Pore-Domain K$^+$ Channels. *Mol. Pharmacol.* **2006**, *69*, 1024–1032. [CrossRef] [PubMed]

130. Guo, Z.; Cao, Y.Q. Over-expression of TRESK K(+) channels reduces the excitability of trigeminal ganglion nociceptors. *PLoS ONE* **2014**, *9*, e87029. [CrossRef]

131. Kang, D.; Mariash, E.; Kim, D. Functional expression of TRESK-2, a new member of the tandem-pore K+ channel family. *J. Biol. Chem.* **2004**, *279*, 28063–28070. [CrossRef] [PubMed]

132. Cotten, J.F. TASK-1 (KCNK3) and TASK-3 (KCNK9) tandem pore potassium channel antagonists stimulate breathing in isoflurane-anesthetized rats. *Anesth. Analg.* **2013**, *116*, 810–816. [CrossRef]

133. Lambert, M.; Mendes-Ferreira, P.; Ghigna, M.R.; LeRibeuz, H.; Adão, R.; Boet, A.; Capuano, V.; Rucker-Martin, C.; Brás-Silva, C.; Quarck, R.; et al. Kcnk3 Dysfunction Exaggerates The Development Of Pulmonary Hypertension Induced By Left Ventricular Pressure Overload. *Cardiovasc. Res.* **2021**. [CrossRef] [PubMed]

134. Heidecker, B.; Lamirault, G.; Kasper, E.K.; Wittstein, I.S.; Champion, H.C.; Breton, E.; Russell, S.D.; Hall, J.; Kittleson, M.M.; Baughman, K.L.; et al. The gene expression profile of patients with new-onset heart failure reveals important gender-specific differences. *Eur. Heart J.* **2010**, *31*, 1188–1196. [CrossRef] [PubMed]

135. Bouter, S.L.; Harchi, A.E.; Marionneau, C.; Bellocq, C.; Chambellan, A.; Veen, T.v.; Boixel, C.; Gavillet, B.; Abriel, H.; Quang, K.L.; et al. Long-Term Amiodarone Administration Remodels Expression of Ion Channel Transcripts in the Mouse Heart. *Circulation* **2004**, *110*, 3028–3035. [CrossRef]

136. Ma, L.; Zhang, X.; Chen, H. TWIK-1 two-pore domain potassium channels change ion selectivity and conduct inward leak sodium currents in hypokalemia. *Sci. Signal.* **2011**, *4*, ra37. [CrossRef] [PubMed]

137. Plant, L.D.; Zuniga, L.; Araki, D.; Marks, J.D.; Goldstein, S.A.N. SUMOylation Silences Heterodimeric TASK Potassium Channels Containing K2P1 Subunits in Cerebellar Granule Neurons. *Sci. Signal.* **2012**, *5*, ra84. [CrossRef]

138. Hwang, E.M.; Kim, E.; Yarishkin, O.; Woo, D.H.; Han, K.-S.; Park, N.; Bae, Y.; Woo, J.; Kim, D.; Park, M. A disulphide-linked heterodimer of TWIK-1 and TREK-1 mediates passive conductance in astrocytes. *Nat. Commun.* **2014**, *5*, 1–15. [CrossRef]

139. Choi, J.H.; Yarishkin, O.; Kim, E.; Bae, Y.; Kim, A.; Kim, S.C.; Ryoo, K.; Cho, C.H.; Hwang, E.M.; Park, J.Y. TWIK-1/TASK-3 heterodimeric channels contribute to the neurotensin-mediated excitation of hippocampal dentate gyrus granule cells. *Exp. Mol. Med.* **2018**, *50*, 1–13. [CrossRef]

140. Reyes, R.; Duprat, F.; Lesage, F.; Fink, M.; Salinas, M.; Farman, N.; Lazdunski, M. Cloning and expression of a novel pH-sensitive two pore domain K+ channel from human kidney. *J. Biol. Chem.* **1998**, *273*, 30863–30869. [CrossRef]

141. Feliciangeli, S.; Chatelain, F.C.; Bichet, D.; Lesage, F. The family of K2P channels: Salient structural and functional properties. *J. Physiol.* **2015**, *593*, 2587–2603. [CrossRef]

142. Maingret, F.; Patel, A.J.; Lesage, F.; Lazdunski, M.; Honoré, E. Mechano- or acid stimulation, two interactive modes of activation of the TREK-1 potassium channel. *J. Biol. Chem.* **1999**, *274*, 26691–26696. [CrossRef]

143. Patel, A.J.; Honoré, E.; Lesage, F.; Fink, M.; Romey, G.; Lazdunski, M. Inhalational anesthetics activate two-pore-domain background K+ channels. *Nat. Neurosci.* **1999**, *2*, 422–426. [CrossRef] [PubMed]

144. Patel, A.J.; Honoré, E.; Maingret, F.; Lesage, F.; Fink, M.; Duprat, F.; Lazdunski, M. A mammalian two pore domain mechano-gated S-like K+ channel. *EMBO J.* **1998**, *17*, 4283–4290. [CrossRef] [PubMed]

145. Levitz, J.; Royal, P.; Comoglio, Y.; Wdziekonski, B.; Schaub, S.; Clemens, D.M.; Isacoff, E.Y.; Sandoz, G. Heterodimerization within the TREK channel subfamily produces a diverse family of highly regulated potassium channels. *Proc. Natl. Acad. Sci. USA* **2016**, *113*, 4194–4199. [CrossRef]

146. Blin, S.; Ben Soussia, I.; Kim, E.-J.; Brau, F.; Kang, D.; Lesage, F.; Bichet, D. Mixing and matching TREK/TRAAK subunits generate heterodimeric K$_{2P}$ channels with unique properties. *Proc. Natl. Acad. Sci. USA* **2016**, *113*, 4200–4205. [CrossRef] [PubMed]

147. Wang, W.; Zhang, M.; Li, P.; Yuan, H.; Feng, N.; Peng, Y.; Wang, L.; Wang, X. An increased TREK-1-like potassium current in ventricular myocytes during rat cardiac hypertrophy. *J. Cardiovasc. Pharm.* **2013**, *61*, 302–310. [CrossRef] [PubMed]

148. Kelly, D.; Mackenzie, L.; Hunter, P.; Smaill, B.; Saint, D. Gene expression of stretch-activated channels and mechanoelectric feedback in the heart. *Clin. Exp. Pharmacol. Physiol.* **2006**, *33*, 642–648. [CrossRef] [PubMed]

149. Kennard, L.E.; Chumbley, J.R.; Ranatunga, K.M.; Armstrong, S.J.; Veale, E.L.; Mathie, A. Inhibition of the human two-pore domain potassium channel, TREK-1, by fluoxetine and its metabolite norfluoxetine. *Br. J. Pharmacol.* **2005**, *144*, 821–829. [CrossRef]

150. Kim, E.J.; Lee, D.K.; Hong, S.G.; Han, J.; Kang, D. Activation of TREK-1, but Not TREK-2, Channel by Mood Stabilizers. *Int. J. Mol. Sci.* **2017**, *18*, 2460. [CrossRef]

151. Schmidt, C.; Wiedmann, F.; Schweizer, P.A.; Becker, R.; Katus, H.A.; Thomas, D. Class I antiarrhythmic drugs inhibit human cardiac two-pore-domain K(+) (K2$_2$p) channels. *Eur. J. Pharm.* **2013**, *721*, 237–248. [CrossRef]

152. Froese, A.; Breher, S.S.; Waldeyer, C.; Schindler, R.F.R.; Nikolaev, V.O.; Rinné, S.; Wischmeyer, E.; Schlueter, J.; Becher, J.; Simrick, S.; et al. Popeye domain containing proteins are essential for stress-mediated modulation of cardiac pacemaking in mice. *J. Clin. Investig.* **2012**, *122*, 1119–1130. [CrossRef]

153. Kirchmaier, B.C.; Poon, K.L.; Schwerte, T.; Huisken, J.; Winkler, C.; Jungblut, B.; Stainier, D.Y.; Brand, T. The Popeye domain containing 2 (popdc2) gene in zebrafish is required for heart and skeletal muscle development. *Dev. Biol.* **2012**, *363*, 438–450. [CrossRef]

154. Simrick, S.; Schindler, R.F.; Poon, K.-L.; Brand, T. Popeye domain-containing proteins and stress-mediated modulation of cardiac pacemaking. *Trends Cardiovasc. Med.* **2013**, *23*, 257–263. [CrossRef] [PubMed]

155. Schindler, R.F.; Scotton, C.; Zhang, J.; Passarelli, C.; Ortiz-Bonnin, B.; Simrick, S.; Schwerte, T.; Poon, K.L.; Fang, M.; Rinné, S.; et al. POPDC1(S201F) causes muscular dystrophy and arrhythmia by affecting protein trafficking. *J. Clin. Invest.* **2016**, *126*, 239–253. [CrossRef] [PubMed]

156. Decher, N.; Kiper, A.K.; Rinné, S. Stretch-activated potassium currents in the heart: Focus on TREK-1 and arrhythmias. *Prog. Biophys. Mol. Biol.* **2017**, *130*, 223–232. [CrossRef] [PubMed]

157. Peyronnet, R.; Nerbonne, J.M.; Kohl, P. Cardiac Mechano-Gated Ion Channels and Arrhythmias. *Circ. Res.* **2016**, *118*, 311–329. [CrossRef]

158. Decher, N.; Ortiz-Bonnin, B.; Friedrich, C.; Schewe, M.; Kiper, A.K.; Rinné, S.; Seemann, G.; Peyronnet, R.; Zumhagen, S.; Bustos, D.; et al. Sodium permeable and "hypersensitive" TREK-1 channels cause ventricular tachycardia. *EMBO Mol. Med.* **2017**, *9*, 403–414. [CrossRef]

159. Abraham, D.M.; Lee, T.E.; Watson, L.J.; Mao, L.; Chandok, G.; Wang, H.-G.; Frangakis, S.; Pitt, G.S.; Shah, S.H.; Wolf, M.J.; et al. The two-pore domain potassium channel TREK-1 mediates cardiac fibrosis and diastolic dysfunction. *J. Clin. Investig.* **2018**, *128*, 4843–4855. [CrossRef]

160. Seyler, C.; Schweizer, P.A.; Zitron, E.; Katus, H.A.; Thomas, D. Vernakalant activates human cardiac K(2P)17.1 background K(+) channels. *Biochem. Biophys. Res. Commun.* **2014**, *451*, 415–420. [CrossRef]

161. Gierten, J.; Ficker, E.; Bloehs, R.; Schlömer, K.; Kathöfer, S.; Scholz, E.; Zitron, E.; Kiesecker, C.; Bauer, A.; Becker, R.; et al. Regulation of two-pore-domain (K2P) potassium leak channels by the tyrosine kinase inhibitor genistein. *Br. J. Pharm.* **2008**, *154*, 1680–1690. [CrossRef]

162. Wiedmann, F.; Beyersdorf, C.; Zhou, X.-B.; Kraft, M.; Foerster, K.I.; El-Battrawy, I.; Lang, S.; Borggrefe, M.; Haefeli, W.E.; Frey, N. The Experimental TASK-1 Potassium Channel Inhibitor A293 Can Be Employed for Rhythm Control of Persistent Atrial Fibrillation in a Translational Large Animal Model. *Front. Physiol.* **2021**, *11*, 1869. [CrossRef]

163. Liang, B.; Soka, M.; Christensen, A.H.; Olesen, M.S.; Larsen, A.P.; Knop, F.K.; Wang, F.; Nielsen, J.B.; Andersen, M.N.; Humphreys, D.; et al. Genetic variation in the two-pore domain potassium channel, TASK-1, may contribute to an atrial substrate for arrhythmogenesis. *J. Mol. Cell Cardiol.* **2014**, *67*, 69–76. [CrossRef]

164. Wirth, K.J.; Brendel, J.; Steinmeyer, K.; Linz, D.K.; Rütten, H.; Gögelein, H. In vitro and in vivo effects of the atrial selective antiarrhythmic compound AVE1231. *J. Cardiovasc. Pharm.* **2007**, *49*, 197–206. [CrossRef]

165. Knobloch, K.; Brendel, J.; Peukert, S.; Rosenstein, B.; Busch, A.E.; Wirth, K.J. Electrophysiological and antiarrhythmic effects of the novel I(Kur) channel blockers, S9947 and S20951, on left vs. right pig atrium in vivo in comparison with the I(Kr) blockers dofetilide, azimilide, d,l-sotalol and ibutilide. *Naunyn Schmiedebergs Arch. Pharm.* **2002**, *366*, 482–487. [CrossRef]

166. Manichaikul, A.; Rich, S.S.; Allison, M.A.; Guagliardo, N.A.; Bayliss, D.A.; Carey, R.M.; Barrett, P.Q. KCNK3 Variants Are Associated With Hyperaldosteronism and Hypertension. *Hypertension* **2016**, *68*, 356–364. [CrossRef] [PubMed]

167. Gerstin, K.M.; Gong, D.H.; Abdallah, M.; Winegar, B.D.; Eger, E.I.I.; Gray, A.T. Mutation of KCNK5 or Kir3.2 Potassium Channels in Mice Does Not Change Minimum Alveolar Anesthetic Concentration. *Anesth. Analg.* **2003**, *96*, 1345–1349. [CrossRef]

168. Lloyd, E.E.; Crossland, R.F.; Phillips, S.C.; Marrelli, S.P.; Reddy, A.K.; Taffet, G.E.; Hartley, C.J.; Bryan, R.M., Jr. Disruption of K(2P)6.1 produces vascular dysfunction and hypertension in mice. *Hypertension* **2011**, *58*, 672–678. [CrossRef]

169. Lloyd, E.E.; Pandit, L.M.; Crossland, R.F.; Marrelli, S.P.; Bryan, R.M., Jr. Endothelium-dependent relaxations in the aorta from K(2p)6.1 knockout mice. *Am. J. Physiol. Regul. Integr. Comp. Physiol.* **2013**, *305*, R60–R67. [CrossRef] [PubMed]

170. Pandit, L.M.; Lloyd, E.E.; Reynolds, J.O.; Lawrence, W.S.; Reynolds, C.; Wehrens, X.H.; Bryan, R.M. TWIK-2 channel deficiency leads to pulmonary hypertension through a rho-kinase-mediated process. *Hypertension* **2014**, *64*, 1260–1265. [CrossRef] [PubMed]

171. Yost, C.S.; Oh, I.; Eger, E.I., 2nd; Sonner, J.M. Knockout of the gene encoding the K(2P) channel KCNK7 does not alter volatile anesthetic sensitivity. *Behav. Brain Res.* **2008**, *193*, 192–196. [CrossRef]

172. Mirkovic, K.; Palmersheim, J.; Lesage, F.; Wickman, K. Behavioral characterization of mice lacking Trek channels. *Front. Behav. Neurosci.* **2012**, *6*, 60. [CrossRef]

173. Niemeyer, M.I.; Cid, L.P.; Barros, L.F.; Sepúlveda, F.V. Modulation of the two-pore domain acid-sensitive K+ channel TASK-2 (KCNK5) by changes in cell volume. *J. Biol. Chem.* **2001**, *276*, 43166–43174. [CrossRef]

174. Gray, A.T.; Zhao, B.B.; Kindler, C.H.; Winegar, B.D.; Mazurek, M.J.; Xu, J.; Chavez, R.A.; Forsayeth, J.R.; Yost, C.S. Volatile anesthetics activate the human tandem pore domain baseline K+ channel KCNK5. *Anesthesiology* **2000**, *92*, 1722–1730. [CrossRef] [PubMed]

175. Lambert, M.; Capuano, V.; Boet, A.; Tesson, L.; Bertero, T.; Nakhleh, M.K.; Remy, S.; Anegon, I.; Pechoux, C.; Hautefort, A.; et al. Characterization of Kcnk3-Mutated Rat, a Novel Model of Pulmonary Hypertension. *Circ. Res.* **2019**, *125*, 678–695. [CrossRef]

176. Knobloch, K.; Brendel, J.; Rosenstein, B.; Bleich, M.; Busch, A.E.; Wirth, K.J. Atrial-selective antiarrhythmic actions of novel Ikur vs. Ikr, Iks, and IKAch class Ic drugs and beta blockers in pigs. *Med. Sci. Monit.* **2004**, *10*, Br221–Br228.

177. Peyronnet, R.; Ravens, U. Atria-selective antiarrhythmic drugs in need of alliance partners. *Pharm. Res.* **2019**, *145*, 104262. [CrossRef]

178. Olschewski, A.; Li, Y.; Tang, B.; Hanze, J.R.; Eul, B.; Bohle, R.M.; Wilhelm, J.; Morty, R.E.; Brau, M.E.; Weir, E.K. Impact of TASK-1 in human pulmonary artery smooth muscle cells. *Circ. Res.* **2006**, *98*, 1072–1080. [CrossRef] [PubMed]

179. Ma, L.; Roman-Campos, D.; Austin, E.D.; Eyries, M.; Sampson, K.S.; Soubrier, F.; Germain, M.; Trégouët, D.A.; Borczuk, A.; Rosenzweig, E.B.; et al. A novel channelopathy in pulmonary arterial hypertension. *N. Engl. J. Med.* **2013**, *369*, 351–361. [CrossRef]

180. Davies, L.A.; Hu, C.; Guagliardo, N.A.; Sen, N.; Chen, X.; Talley, E.M.; Carey, R.M.; Bayliss, D.A.; Barrett, P.Q. TASK channel deletion in mice causes primary hyperaldosteronism. *Proc. Natl. Acad. Sci. USA* **2008**, *105*, 2203–2208. [CrossRef]

181. West, J.D.; Austin, E.D.; Rizzi, E.M.; Yan, L.; Tanjore, H.; Crabtree, A.L.; Moore, C.S.; Muthian, G.; Carrier, E.J.; Jacobson, D.A.; et al. KCNK3 Mutation Causes Altered Immune Function in Pulmonary Arterial Hypertension Patients and Mouse Models. *Int. J. Mol. Sci.* **2021**, *22*, 5014. [CrossRef]

182. Heurteaux, C.; Guy, N.; Laigle, C.; Blondeau, N.; Duprat, F.; Mazzuca, M.; Lang-Lazdunski, L.; Widmann, C.; Zanzouri, M.; Romey, G.; et al. TREK-1, a K+ channel involved in neuroprotection and general anesthesia. *EMBO J.* **2004**, *23*, 2684–2695. [CrossRef] [PubMed]

183. Laigle, C.; Confort-Gouny, S.; Le Fur, Y.; Cozzone, P.J.; Viola, A. Deletion of TRAAK potassium channel affects brain metabolism and protects against ischemia. *PLoS ONE* **2012**, *7*, e53266. [CrossRef] [PubMed]

184. Kindler, C.H.; Paul, M.; Zou, H.; Liu, C.; Winegar, B.D.; Gray, A.T.; Yost, C.S. Amide local anesthetics potently inhibit the human tandem pore domain background K+ channel TASK-2 (KCNK5). *J. Pharm. Exp.* **2003**, *306*, 84–92. [CrossRef]

185. Gönczi, M.; Szentandrássy, N.; Johnson, I.T.; Heagerty, A.M.; Weston, A.H. Investigation of the role of TASK-2 channels in rat pulmonary arteries; pharmacological and functional studies following RNA interference procedures. *Br. J. Pharmacol.* **2006**, *147*, 496–505. [CrossRef] [PubMed]

186. Winsvold, B.S.; Bettella, F.; Witoelar, A.; Anttila, V.; Gormley, P.; Kurth, T.; Terwindt, G.M.; Freilinger, T.M.; Frei, O.; Shadrin, A.; et al. Shared genetic risk between migraine and coronary artery disease: A genome-wide analysis of common variants. *PLoS ONE* **2017**, *12*, e0185663. [CrossRef]

187. Shvetsova, A.A.; Gaynullina, D.K.; Schmidt, N.; Bugert, P.; Lukoshkova, E.V.; Tarasova, O.S.; Schubert, R. TASK-1 channel blockade by AVE1231 increases vasocontractile responses and BP in 1- to 2-week-old but not adult rats. *Br. J. Pharm.* **2020**, *177*, 5148–5162. [CrossRef]

188. Bobak, N.; Feliciangeli, S.; Chen, C.C.; Ben Soussia, I.; Bittner, S.; Pagnotta, S.; Ruck, T.; Biel, M.; Wahl-Schott, C.; Grimm, C.; et al. Recombinant tandem of pore-domains in a Weakly Inward rectifying K(+) channel 2 (TWIK2) forms active lysosomal channels. *Sci. Rep.* **2017**, *7*, 649. [CrossRef]

189. Salinas, M.; Reyes, R.; Lesage, F.; Fosset, M.; Heurteaux, C.; Romey, G.; Lazdunski, M. Cloning of a new mouse two-P domain channel subunit and a human homologue with a unique pore structure. *J. Biol. Chem.* **1999**, *274*, 11751–11760. [CrossRef]

190. Berg, A.P.; Talley, E.M.; Manger, J.P.; Bayliss, D.A. Motoneurons express heteromeric TWIK-related acid-sensitive K+ (TASK) channels containing TASK-1 (KCNK3) and TASK-3 (KCNK9) subunits. *J. Neurosci.* **2004**, *24*, 6693–6702. [CrossRef]

191. Kim, D.; Cavanaugh, E.J.; Kim, I.; Carroll, J.L. Heteromeric TASK-1/TASK-3 is the major oxygen-sensitive background K+ channel in rat carotid body glomus cells. *J. Physiol.* **2009**, *587*, 2963–2975. [CrossRef]

192. Zadeh, N.; Graham, J.M., Jr. KCNK9 Imprinting Syndrome. In *GeneReviews(®)*; Adam, M.P., Ardinger, H.H., Pagon, R.A., Wallace, S.E., Bean, L.J.H., Mirzaa, G., Amemiya, A., Eds.; University of Washington: Seattle, WA, USA, 2017.

193. Yost, C.S. A new look at the respiratory stimulant doxapram. *CNS Drug Rev.* **2006**, *12*, 236–249. [CrossRef] [PubMed]

194. Chatelain, F.C.; Bichet, D.; Feliciangeli, S.; Larroque, M.M.; Braud, V.M.; Douguet, D.; Lesage, F. Silencing of the tandem pore domain halothane-inhibited K+ channel 2 (THIK2) relies on combined intracellular retention and low intrinsic activity at the plasma membrane. *J. Biol. Chem.* **2013**, *288*, 35081–35092. [CrossRef]

195. Graff, S.M.; Johnson, S.R.; Leo, P.J.; Dadi, P.K.; Dickerson, M.T.; Nakhe, A.Y.; McInerney-Leo, A.M.; Marshall, M.; Zaborska, K.E.; Schaub, C.M.; et al. A KCNK16 mutation causing TALK-1 gain of function is associated with maturity-onset diabetes of the young. *JCI Insight* **2021**, *6*, e138057. [CrossRef]

196. Suzuki, Y.; Tsutsumi, K.; Miyamoto, T.; Yamamura, H.; Imaizumi, Y. Heterodimerization of two pore domain K+ channel TASK1 and TALK2 in living heterologous expression systems. *PLoS ONE* **2017**, *12*, e0186252. [CrossRef] [PubMed]

197. Domingues-Montanari, S.; Fernández-Cadenas, I.; Del Río-Espinola, A.; Mendioroz, M.; Fernandez-Morales, J.; Corbeto, N.; Delgado, P.; Ribó, M.; Rubiera, M.; Obach, V.; et al. KCNK17 genetic variants in ischemic stroke. *Atherosclerosis* **2010**, *208*, 203–209. [CrossRef] [PubMed]

198. Grabauskas, G.; Wu, X.; Zhou, S.; Li, J.; Gao, J.; Owyang, C. High-fat diet-induced vagal afferent dysfunction via upregulation of 2-pore domain potassium TRESK channel. *JCI Insight* **2019**, *4*, e130402. [CrossRef] [PubMed]

199. Park, H.; Kim, E.J.; Ryu, J.H.; Lee, D.K.; Hong, S.G.; Han, J.; Han, J.; Kang, D. Verapamil Inhibits TRESK (K(2P)18.1) Current in Trigeminal Ganglion Neurons Independently of the Blockade of Ca(2+) Influx. *Int. J. Mol. Sci.* **2018**, *19*, 1961. [CrossRef]

200. Enyedi, P.; Czirják, G. Properties, regulation, pharmacology, and functions of the K2P channel, TRESK. *Pflügers Arch. Eur. J. Physiol.* **2015**, *467*, 945–958. [CrossRef]